Cell Communication and Signaling

RESEARCH

Open Access

A comparative proteomic, transcriptomic and glycomic analysis of extracellular vesicle isolation techniques highlights ExoGAG efficiency for a more complete identification of breast milk molecular signaling pathways

María Pereira-Hernández[1,2,3†], Rosaura Picáns-Leis[4†], María E. Vázquez-Mosquera[4†], Nerea Lago-Baameiro[5,6,7], Pedro Fortes-González[1,2,3], Laura López-Valverde[4], Ana Barcia de la Iglesia[1,2,3], Laura Núñez-González[1,2,3], Susana B. Bravo[8], María Pardo[5,6,7], María L. Couce[4*] and Miguel A. Garcia-Gonzalez[1,2,3*]

Abstract

Background Human milk (HM) is the first form of communication between mothers and newborns and it is implicated in the infant growth and protection. We recently showed a functional characterization of HM, unmasking the molecular mechanisms related to EVs signaling and its functional role in prematurity. In that study, we identified the need to establish and optimize a standard isolation protocol for human milk extracellular vesicles (mEVs).

Methods Four mEVs isolation methods were compared: ultracentrifugation (UC), size exclusion chromatography (SEC), immunoprecipitation with tetraspanin CD9 (IP_CD9) and ExoGAG. Three pools of human milk (each composed of samples from ten donor mothers) were used and isolation of mEVs was performed starting from the same volume for each method. The proteomic, transcriptomic and glycomic composition of the extracellular vesicles obtained after isolation was then analyzed for each method. The sensitivity, specificity and quality of the results were also determined. A comparative analysis of results common across all isolation methods was performed to identify potential signaling pathways associated with mEVs.

Results ExoGAG and UC proved to be the most efficient of the four techniques compared for mEVs isolation. However, ExoGAG compared to UC provided a higher concentration of total and vesicle-related proteins and peptides and a higher glycoprotein count keeping all the glycan subgroups. Despite ExoGAG and UC show similar vesicle

†María Pereira-Hernández, Rosaura Picáns-Leis and María E. Vázquez-Mosquera contributed equally to this work.

*Correspondence:
María L. Couce
maria.luz.couce.pico@sergas.es
Miguel A. Garcia-Gonzalez
miguel.garcia.gonzalez@sergas.es

Full list of author information is available at the end of the article

profiles in terms of size, concentration, tetraspanin subpopulations and EVs markers, ExoGAG was the most efficient technique in terms of accuracy, consistency and reproducibility for omics studies. Furthermore, results allowed us to identify that mEVs components are involved in the signaling pathways of infant biological development, immune system maturation and protein metabolism.

Conclusions This study establishes UC and ExoGAG as reliable methods for mEVs isolation and describes its protocol, being ExoGAG the most efficient. Also, the omics analysis show that biomolecules conforming those mEVs are linked to the defense system against external agents (specific role in the immune system pathway) and in the correct establishment of the neural structure (developmental pathway), while providing all the nutritional requirements for the correct growth of the newborn (metabolic pathway).

Keywords Extracellular vesicles, Human milk, Isolation method, Proteomics, Transcriptomics, Glycomics

Graphical Abstract

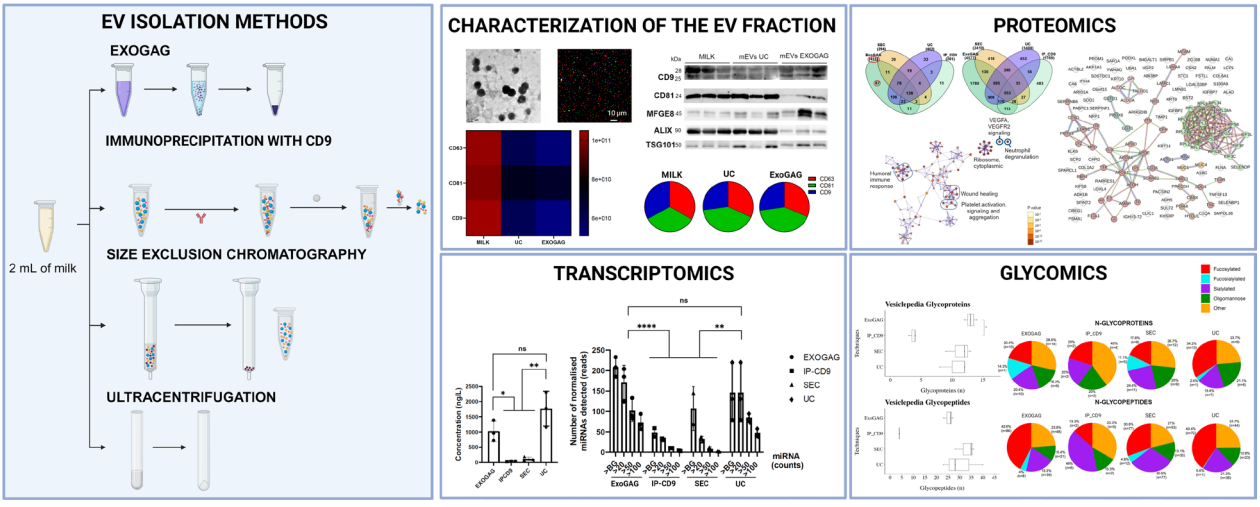

Background

Human milk is an enriched and dynamic fluid which changes its composition through the lactation period [10]. This biofluid is the first form of communication between mothers and newborns and it is implicated in the infant growth and protection [18]. Among its composition, we can find a wide range of molecules, such proteins, lipids and extracellular vesicles (EVs) [4, 10, 57, 70]. EVs are described as a group of lipid membrane-bound structures loaded with various bioactive molecules like proteins, lipids and nucleic acids [64] released from diverse cells into the extracellular space [27]. At first, EVs were thought to serve as an alternative pathway for getting rid of cellular waste. However, they are now known to play a very important role in maintaining cellular homeostasis, acting as packaging, transport and delivery devices for molecules between cells [56]. EVs are shed by most cell types under physiological and pathological conditions, although stress conditions can alter both increasing or decreasing its release [40]. They also reflect specific characteristics identical to their cells of origin, with cell-specific proteins, lipids, non-coding RNA and all subtypes of coding RNA, and even reflecting same expression levels [49, 66, 28]. These vesicles can be isolated by almost all sorts of biological fluids (serum, plasma, urine, breast milk, cerebrospinal fluid, saliva, among others) [66]. For this reason, the study of extracellular vesicles recently became a topic of interest in biomedical research as they are present in a high number of biological samples and they reflect the status of the cell they are shed from [5].

Glycosylation is a key post-translational modification implicated in a wide range of metabolic diseases [68]. EVs are heavily glycosylated with a variety of glycosaminoglycans (GAGs), vital components for EVs biogenesis and internalization processes [5, 8, 52]. More than 70% of human milk proteins are glycosylated, playing an important role in cell-cell adhesion and ligand binding, among other roles [34]. Taking advantage of a cationic colorant that binds specifically to GAGs, our group have developed an isolation method (patent application P201531297, PCT/ES2016/070637; product ExoGAG, Licenced by Nexothech) that specifically isolates the glycosylated fraction bound to GAGs, including glycoproteins and vesicular fraction. ExoGAG is an easy-to-use and highly specific EVs isolation technology for the

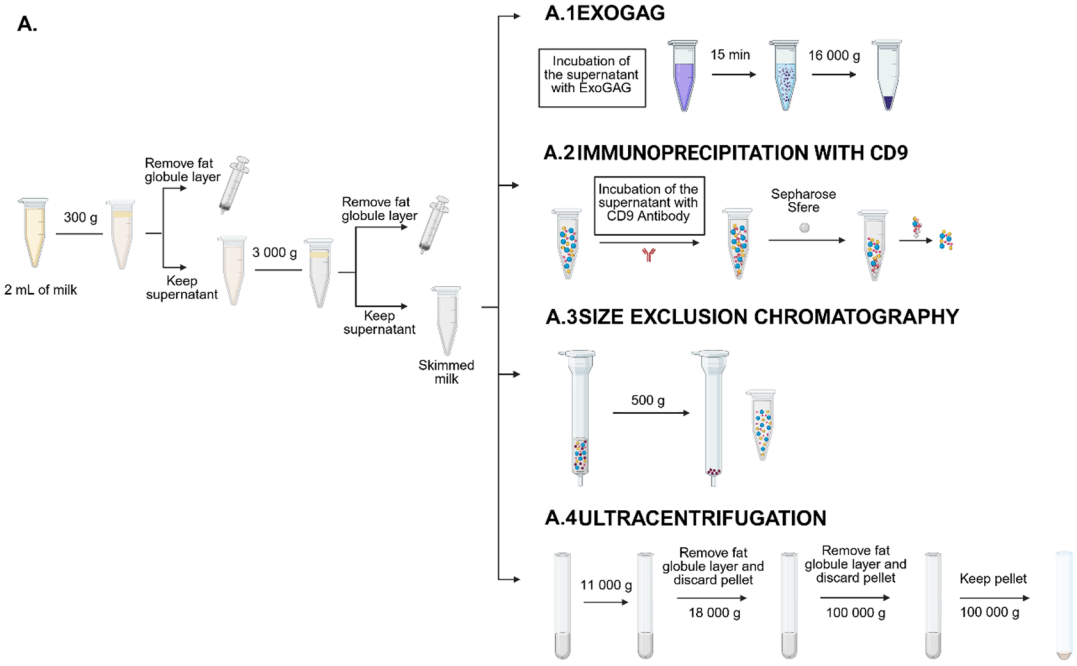

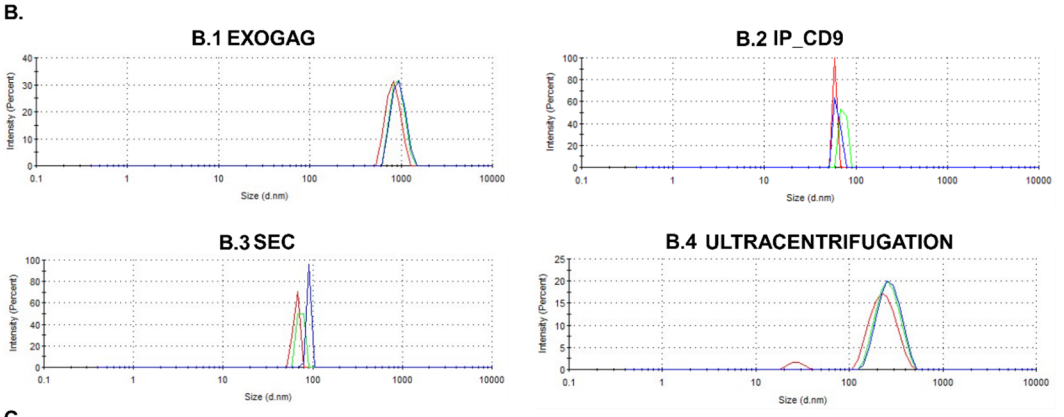

C.

EV markers ExoGAG	
Transmembrane or GPI-anchored proteins	CD9
	CD47
	ITGA
	ITGB
	TFR2
	SDC
	BSG
	CD59
Cytosolic	CHMP1A
	CHMP2A
	PDCD6IP
	VPS4B
	SDCBP
	HSPA8
	HSP90AB1
	ACTB
	TUBA1A
	TUBA1B
	TUBA1C
	TUBA3C
	TUBA3D
	TUBA3E
	TUBB8B
	TUBB
	TUBB2A
	TUBB2B
	TUBB4A
	TUBB4B
	TUBB6
	TUBB8
	GAPDH

EV markers IPCD9	
Transmembrane or GPI-anchored proteins	CD59
Cytosolic	HSPA8
	ACTB
	TUBB8B
	TUBB
	TUBB2A
	TUBB2B
	TUBB4A
	TUBB4B
	TUBB6
	TUBB8
	GAPDH

EV markers SEC	
Transmembrane or GPI-anchored proteins	CD63
	SDC4
	BSG
	CD59
Cytosolic	CHMP1A
	CHMP1B
	CHMP2A
	CHMP4B
	VPS4A
	VPS4B
	SDCBP
	ACTB
	TUBA1A
	TUBA1B
	TUBA1C
	TUBB
	GAPDH

EV markers UC	
Transmembrane or GPI-anchored proteins	CD9
	CD63
	CD81
	CD82
	SDC4
	BSG
	CD59
Cytosolic	CHMP1A
	CHMP1B
	CHMP2A
	PDCD6IP
	VPS4A
	VPS4B
	SDCBP
	HSPA8
	HSP90AB1
	ACTB
	TUBA1A
	TUBA1B
	TUBA1C
	TUBA3C
	TUBA3D
	TUBA3E
	TUBB8B
	TUBB
	TUBB2A
	TUBB2B
	TUBB4A
	TUBB4B
	TUBB6
	TUBB8
	GAPDH

Fig. 1 (See legend on next page.)

(See figure on previous page.)

Fig. 1 Scheme of milk extracellular vesicles isolation techniques and brief characterization. (**A**) Milk EVs isolation by A.1) Ultracentrifugation A.2) Immunoprecipitation with CD9, A.3) Size Exclusion Chromatography and A.4) ExoGAG. (**B**) Size and distribution profiles of B.1) UC, B.2) IP_CD9, B.3) SEC and B.4) ExoGAG mEVs with Zetasizer. (**C**) EVs markers according to MISEV 2023 found in every technique DDA mass spectrometry data. Prior to extracellular vesicle isolation, milk samples were organized in three pools (POOL1, POOL2 and POOL3) and went through an initial defatting step with two serial centrifugations. Then, every pool went through an isolation process with Ultracentrifugation, Immunoprecipitation, Size Exclusion Chromatography and ExoGAG. A brief characterization was developed to determine size, distribution and EVs marker composition of each method

analysis of different cargos, such as EVs-proteome, EVs-DNA, EVs-RNA, EVs-miRNA sequencing and expression detection, from different biofluids like serum, plasma, urine and sperm [24–26, 44]. Recently, we have published the first study to show a complete functional characterization of human milk using ExoGAG (proteome and miRNA derived from the same three initial pools of samples with similar starting volume – 2 mL-), unmasking the molecular mechanisms related to EVs and their functional role in prematurity [48]. Now, this study aims to compare, according to the MISEV2023 guidelines [63], the most commonly used techniques with ExoGAG performance for isolation and characterization of the proteome, transcriptome and glycosignature of vesicles from human milk samples.

Methods

Human milk samples

Human milk samples ($n = 30$) were collected from mothers one month after delivery and organized into three pools of samples and frozen (POOL1, POOL2, POOL3). Mature breast milk was used as breastfeeding was already well established in this period. 30 human milk samples were collected by manual expression early in the morning. Mothers aged > 18 years of term children (37–41 weeks gestational age). Exclusion criteria included maternal illnesses that could potentially modify miRNA profile cancer, hypertension, obesity, autoimmune illnesses, toxic consumption, restrictive diets and mothers of children with serious pathologies or malformations. Anthropometric data and specific characteristics of the mothers and newborns included in the study are described in Supplementary Table 1. Each pool consisted of ten samples and had a similar final volume (~ 235 ml). Milk pools were thaw on ice and several defatting steps were performed prior to EVs isolation. 2 mL of pools were centrifuged at 300 g for 10 min at 4 °C to remove the fat globule layer. A second centrifugation at 3000 g for 10 min at 4 °C was performed with the same purpose. Participating mothers gave informed consent to participate in this study. Ethics committee approval was obtained from Research Ethics Committees of Galicia (register code: 2020/243).

Milk extracellular vesicles (mEVs) isolation

EVs from the three pools were isolated from an initial volume of two milliliters with all the isolation methods. For all the techniques further developed (characterization of the EVs component and omics) comparisons between techniques correspond to EVs from 2 mL of each pool of milk isolated by the four methods.

Ultracentrifugation

Minor modifications were performed from an Ultracentrifugation (UC) protocol for plasma EVs isolation [6] so that we could decrease the required isolation volume from ~ 24 mL down to 2 mL. UC was performed in the Beckman Coulter OptimaTM-100XP ultracentrifuge with the SW41Ti swing-bucket rotor, 13,2 mL tubes (Thinwall Polypropylene Tubes, 14 × 89 mm; #331362 Beckman Coulter), an acceleration/deceleration brake profile of 9 and a k-factor of 124. The supernatant was discarded and the pellet with the vesicles was resuspended in the corresponding buffer for subsequent experiments. For western blot analysis and proteomics, the pellets were resuspended in 5% and 1% SDS, and for the rest of the characterization in deionized water or 1X PBS. In addition, TRI reagent (Sigma-Aldrich T9424) was used for RNA extraction (Fig. 1A). For detailed information, please refer to Supplementary information section.

Immunoprecipitation with CD9 (IP_CD9)

Two independent immunoprecipitations per sample were performed with the supernatant and finally pooled. 1.5 ug of CD9 antibody (Invitrogen® #10626D) was added to each 750 µL of pool in each Eppendorf and incubated on a rotating wheel at 4 °C overnight. Next day, 15µL of Sepharose spheres (Protein A/G PLUS-Agarose, Santa Cruz Biotechnology Inc® #sc-2003) were added and incubated for 2 h on a rotating wheel at 4 °C. After this time, the samples were washed three times with deionized water, centrifugated for 3 min at 2500 g and supernatant was discarded (Fig. 1B). Finally, samples were resuspended in the corresponding buffer as and centrifugated at 2500 g to eliminate the Sepharose spheres. For western blot analysis and proteomics, the pellets were resuspended in 5% and 1% SDS, and for the rest of the characterization in deionized water or 1X PBS. In addition, TRI reagent (Sigma-Aldrich T9424) was used for RNA extraction. For detailed information, please refer to Supplementary information section.

Size exclusion chromatography (SEC)

Size Exclusion Chromatography was performed with SmartSEC™ Single columns (System Biosciences, Cat #

SSEC200A-1) following manufacturers recommendations (Fig. 1C). The final volume containing EVs was mixed with the corresponding buffer. For western blot analysis and proteomics, the pellets were resuspended in 5% and 1% SDS, and for the rest of the characterization in deionized water or 1X PBS. In addition, TRI reagent (Sigma-Aldrich T9424) was used for RNA extraction. For detailed information, please refer to Supplementary information section.

ExoGAG

Sample was incubated in 1:2 ratio with ExoGAG reagent for 15 min at 4 °C. After incubation, the mix was centrifuged at 16,000 g for 15 min at 4 °C. Next, we discarded the supernatant fraction and resuspended the pellet in the corresponding buffer for the next experiments (Fig. 1D). For western blot analysis and proteomics, the pellets were resuspended in 5% and 1% SDS, and for the rest of the characterization in deionized water or 1X PBS. In addition, TRI reagent (Sigma-Aldrich T9424) was used for RNA extraction. For detailed information, please refer to Supplementary information section.

Dynamic light scattering (DLS)

Size and distribution of mEVs isolated by the four techniques were assessed by DLS with Zetasizer NanoZS (Malvern Instruments, UK). Measurements were performed at RT upon 1/100 dilution with PBS 1X. ZEN0040 cells were used. Three measurements with no delay between them, eleven runs and with a run duration of 10 s were performed. The measurement angle was 173° Backscatter (NIBS Default) and with an equilibration time of 120 s.

Proteomic analysis

Protein extraction and digestion

Proteins contained in mEVs isolated from the four methods were solubilized in 120 µl SDS 5%. Protein concentration was measured with DC™ Protein Assay Kit II (Bio-Rad® #5000112) according to the manufacturing protocol. Protein aliquots of 100 µg were concentrated loaded on a 10% SDS-PAGE gel for trypsin digestion. Once the front penetrated 3 mm into the resolving gel, the run was stopped [7, 17, 37, 51]. The protein band was visualized, with Sypro-Ruby fluorescent staining (Lonza, Porriño, Pontevedra, Spain), excised, and processed for in-gel tryptic digestion following the standard protocol of Shevchenko et al. [54], with minor modifications. 10 mM dithiothreitol (Sigma-Aldrich, St. Louis, MO, USA) in 50 mM ammonium bicarbonate (Sigma-Aldrich, St. Louis, MO, USA) was used for gel pieces reduction and 55 mM iodoacetamide (Sigma-Aldrich, St. Louis, MO, USA) in 50 mM ammonium bicarbonate for alkylation. Pieces were washed with 50 mM ammonium bicarbonate in 50% methanol (HPLC grade, Scharlau, Barcelona, Spain), dehydrated by adding acetonitrile (HPLC grade, Scharlau, Barcelona, Spain), and dried in a SpeedVac. Modified porcine trypsin (Promega, Madison, WI, USA) was added at a concentration of 20 ng/µL in 20 mM ammonium bicarbonate and incubated overnight at 37 °C. Peptides were extracted by three 20 min incubations in 40 µL of 60% acetonitrile in 0.5% HCOOH and stored at −20 °C.

Qualitative LC-MS/MS analysis. Data-dependent acquisition (DDA-MS)

To perform protein identification, reverse phase chromatography was used to separate digested peptides from each sample. The gradient was stablished using a micro liquid chromatography system (Eksigent Technologies nanoLC 400, Sciex, Redwood City, CA, USA) coupled to a high-speed Triple TOF 6600 mass spectrometer (Sciex, Redwood Int. J. Mol. Sci. 2021, 22, 226 18 of 22 City, CA, USA) with a microflow source. We load 4µLof peptide solution form each sample in a Chrom XP C18 silica-based reversed-phase column (150 0.30 mm) with a 3 mm particle size and 120Å pore size (Eksigent, Sciex Redwood City, CA, USA). The trap column was a YMC-TRIART C18 (YMC Technologies Teknokroma Analítica, Barcelona, Spain), with a 3 mm particle size and 120Å pore size. Flow-rate was settled to 5 µl/min under gradient elution conditions, using 0.1% formic acid in water as mobile phase A, and 0.1% formic acid in acetonitrile as mobile phase B. Peptides were separated for 90 min under gradient ranging from 2 to 90% mobile phase B.

Peptides were separated for 90 min under gradient ranging from 2 to 90% mobile phase B with the following gradient: 0–90 min: 2%B, 90–90.1 min: 30%B, 90.1–95 min: 90%B, 95–95.1 min: 90%B, 95.1–100 min: 5%B.

Data acquisition was performed by a TripleTOF 6600 System (Sciex, Foster City, CA) using a data-dependent analysis (DDA-MS) workflow. Source and interface conditions were the following: ionspray voltage floating (ISVF) 5500 V, curtain gas (CUR) 25, collision energy (CE), 10 and ion source gas 1 (GS1) 25. The instrument was operated with Analyst TF 1.7.1 software (Sciex, USA). Switching criteria was set to ions greater than mass to charge ratio (m/z) 350 and smaller than m/z 1400 with charge state of 2–5, mass tolerance of 250 ppm and an abundance threshold of more than 200 counts per second (cps). Previous target precursor ions were excluded for 15 s. The fragmentation ions were generated by ion trap collision-induced dissociation (CID). The instrument was automatically calibrated every 4 h using tryptic peptides from PepCalMix as external calibrant. For detailed information, please refer to Supplementary information section.

Data analysis

Data files were processed using ProteinPilot™ 5.0.1 software from Sciex, with algorithms ParagonTM and ProgroupTM. A Human specific Uniprot database was used database (https://www.uniprot.org/) (*UniProt release 2024_01 With 44413 human proteins*), specifying iodoacetamide at cysteine alkylation as fixed modification and methionine oxidation as variable modification. False discovery rate was performed using a non-lineal fitting method, displaying only those results that reported a 1% Global false discovery rate or better (Li et al., 2021). Reproducibility of biological samples was assesed using the stdev scatter plot obtained from Scaffold 5 (Supplementary Fig. 1). The Stdev Scatterplot provides a method of estimating the coefficient of variation or variance (CV) of the estimates of protein abundance. The figure includes a graph that plots the Log10(Mean) and Log10(Standard Deviation) for each protein appearing in the protein list for the whole data set and categories when no quantitative test is applied [1]. The individual values of DDA-MS spectral counts per technique and sample were used to perform the blox pots. For detailed information, please refer to Supplementary information section.

Quantitative sequential window acquisition of all theoretical fragment ion mass spectra (SWATH-MS) analysis

Generation of the reference spectral library 4 µL of each pool of each group was analyzed by a shotgun data-dependent acquisition (DDA-MS) approach, as previously described but using a 40-minute gradient [35]. For detailed information, please refer to Supplementary information section.

Quantification by SWATH-MS and data analysis The quantitative proteomic analysis was developed with SWATH-MS method in a hybrid quadrupole-TOF mass spectrometer, 6600+ (Sciex, Framingham, MA, USA) (Sciex) according to the published protocol by our group [13, 14] which was modified from [39, 59]. The SWATH–MS acquisition was performed using DIA (Data Independent Acquisition) method. 4 ug of peptides from each mEVs preparation was subjected to chromatographic separation, as described before. The SWATH-MS method is based on repeating a cycle that consisted of the acquisition of 100 TOF MS/MS scans (400 to 1500 m/z, high sensitivity mode, 50 ms acquisition time) of overlapping sequential precursor isolation windows of variable width (1 m/z overlap) covering the 400 to 1250 m/z mass range with a previous TOF MS scan (400 to 1500 m/z, 50 ms acquisition time) for each cycle. Total cycle time was 6.3 s. The fragmentation ions were generated by ion trap collision-induced dissociation (CID). For each sample set, the width of the 100 variable windows was optimized according to the ion density found in the DDA-MS runs using a SWATH-MS variable window calculator worksheet from Sciex.

The targeted data extraction was performed by PeakView (version 2.2) using the SWATH Acquisition MicroApp (version 2.0). To obtain the peak areas, up to ten peptides per protein and seven fragments per peptide were selected based on signal intensity. Shared and modified peptides were excluded. The integrated peak areas (SWATH-MS areas) were directly exported to the MarkerView software (Sciex) for relative quantitative analysis. Integrated peak areas were normalized using MLR normalization [13, 14]. In order to see the reproducibility of the SWATH method across the samples, although we used biological samples replicates not technical replicates a cumulative percentage of analytes versus the percentage coefficient of variation (CV) were plotted. This data likely refers the precision and accuracy of laboratory analysis (Supplementary Fig. 2).

Unsupervised multivariate statistical analysis, using principal component analysis (PCA), was performed. A Student's t-test analysis using the MarkerView software was performed for comparison among the samples. The deregulated proteins were selected using p-value < 0.05 and FC > 1.5 or < 0.6 (or FC > 1.5 or <−1.5) as cut-off. For detailed information, please refer to Supplementary information section.

Functional analysis and network analysis

The differentially expressed proteins (DEPs) were subjected to functional analysis and interpreted through various open access bioinformatics tools for analyzing biological information: Scaffold DDA™ version 6.4.1, Bioinformatics and Evolutionary Genomics (https://bioinformatics.psb.ugent.be/webtools/Venn/), Funrich Version 3.1.3, String Tool (https://string-db.org/), Metascape Tool (https://metascape.org/gp/index.html#/main/step1), Reactome Pathway Database (https://reactome.org/) and SR Plot (https://www.bioinformatics.com.cn/en).

Glycomic analysis

Glycated peptide detection

Output raw files retrieved from Triple TOF 6600 (Sciex, Toronto, Canada) using a DDA-MS method were analyzed on PEAKS 10 Studio Software [20] (Bioinformatics Solutions Inc., Waterloo, Canada) against a Human UniProt database. The peptide mass tolerance was set to 10 ppm and 0.01 Da for MS/MS. Variable modifications selected were those included in the PEAKs PTM Glycosylations database. For high-confidence peptide and protein identification a FDR (False Discovery Rate) of 1% was selected with a minimum of 2 ranked peptides used for peptide filtering.

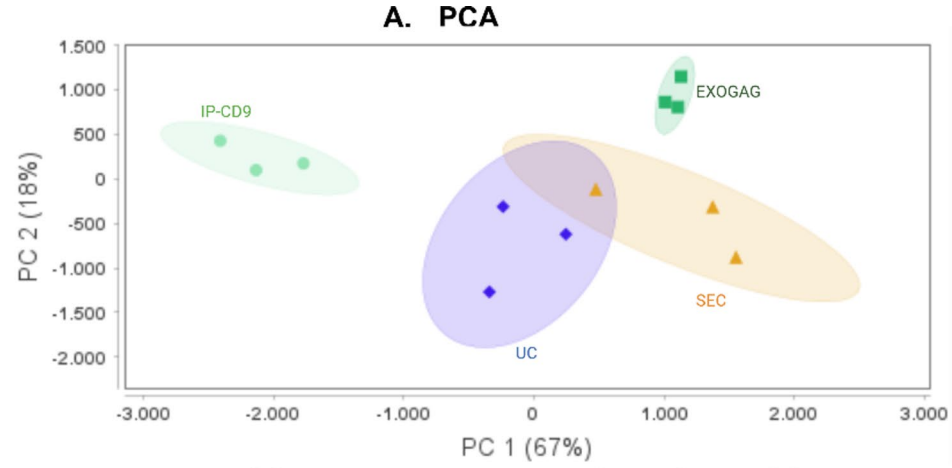

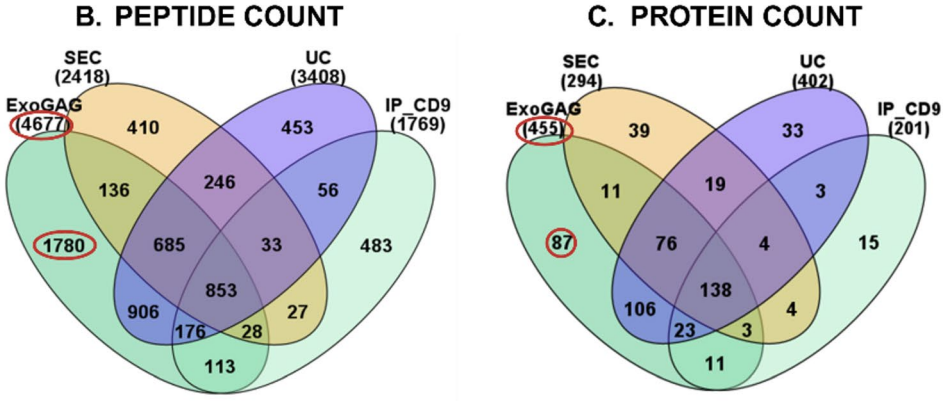

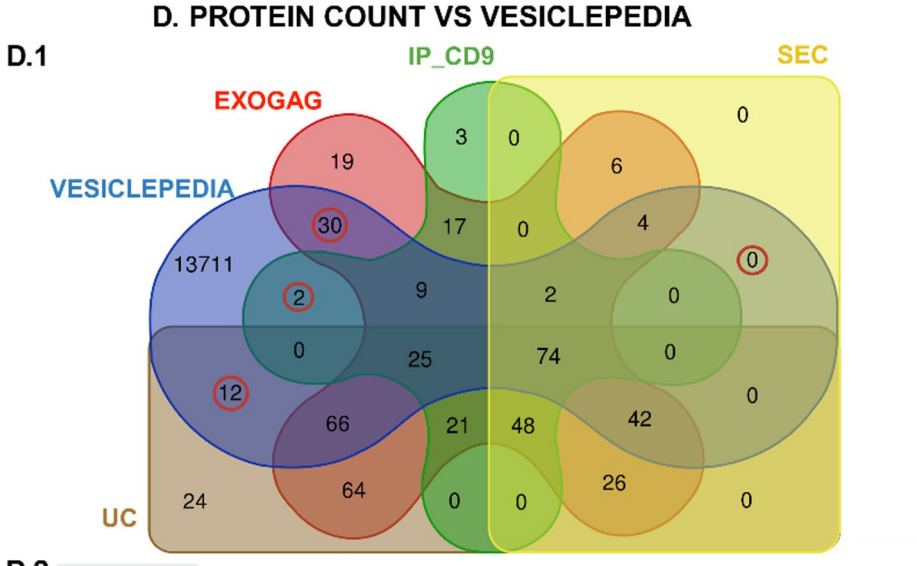

D.2

Vesiclepedia				
ExoGAG	252 (1,8%)			
IP_CD9	112 (0,8%)	196 (42,8%)		
SEC	156 (1,1%)	259 (53,1%)	149 (43,1%)	
UC	219 (1,5%)	366 (74,8%)	168 (38,6%)	237 (51,6%)
	Vesiclepedia	ExoGAG	IP_CD9	SEC

Fig. 2 (See legend on next page.)

(See figure on previous page.)

Fig. 2 DDA-MS recovery analysis. (**A**) PCA analysis of DDA-MS data from mEVs isolated by the four methods. (**B**) Venn Diagram of peptide recovery between methods. (**C**) Venn Diagram of protein recovery between methods. (**D**) Total protein count in comparison to Vesiclepedia database. (D.1) Venn Diagram and (D.2) correlation matrix. Samples are properly clustered in the PCA analysis, which explains more than 75% of the differences between groups with only the first two components (PC1 and PC2). Total peptide and protein count show protein abundance and similarities found between groups. ExoGAG stands out in both cases, also reaching statistical significance in comparison to IP_CD9. Despite not finding significant differences with the other techniques, we can see a tendence where UC and SEC have less power recovery than ExoGAG. Again, in comparison to Vesiclepedia database the greater yield corresponds to ExoGAG

DDA-MS results were ran against UNIMOD for PTM classification. Clusters of glycan types were generated if the PTM field included any of the following UNIMOD Interim Names according to the rules described hereafter: '*dHex*', *'Fucose*', '*Fucosylation'* and *'Biantennary'* were classified as Fucosylations; *'NeuGc'*, *'NeuAc'*, *'Kdn'* and *'Neuraminic acid'* were classified as Syalilations; combinations of the two former groups were classified as a Fucosyalilations; entries not containing any of the above names but the ones *'HexNAc'* or *'N-linked glycan'* were classified as Oligomannoses; every other entry was classified as Other.

Data pre-processing

Data was normalized including only peptides present in Vesiclepedia to focus on EVs-related proteins [9]. Preprocessing of the DDA-MS output data was performed using Python v3.12.4 in Jupyter Notebook v7.0.8 [30] and the following third-party libraries: numpy v1.26.4 [23], pandas v2. 2.2, vulture v2.11 tqdm v4.66.4. For detailed information, please refer to Supplementary information section.

EVs MiRNA analysis

TRI reagent (Sigma-Aldrich T9424) was used for RNA extraction following manufacturer's recommendations. Quantity and quality of the extracted RNA was assessed using a Qubit® 2.0 fluorometer (Thermo Fisher Scientific, Inc.) and an Agilent 2100 Bioanalyzer (Agilent Technologies, Inc.). The NanoString nCounter MAX system (NanoString Technologies®, Inc., Seattle, WA, USA) was used to determine miRNA expression levels in human milk EVs. We used 100–6000 µg of total RNA as input using the commercial nCounter® miRNA v3 Expression Panel assay (https://nanostring.com/products/ncounter-assays-panels/immunology/mirna/). Quality co ntrol (QC) of the raw data was performed following the manufacturer's recommendations. Data normalization was performed using both DESeq2 [38] and RUVSeq [50] packages, as previously described by Bhattacharya et al. [2]. Genes with counts lower than background levels were not included. Differentially expressed miRNAs were identified using the DESeq2 [38] package. For detailed information, please refer to Supplementary information section.

The R package miRNAtap was employed to predict gene targets for the miRNAs included in the nCounter® miRNA v3 Expression Panel assay. The miRNA target prediction was based on five databases: PicTar, DIANA, TargetScan, MiRanda, and miRDB. A geometric mean score was used to rank each gene, and a gene was retained as a target for a given miRNA if it appeared in at least three of the five databases. An over-representation analysis (ORA) based on Gene Ontology (GO) Biological Process terms was conducted for the predicted targets of each miRNA > 100 counts overlapping between samples isolated by the same technique using the ClusterProfiler R package. The Benjamini-Hochberg procedure was applied to correct for multiple testing. Both the P-value and Q-value thresholds were set to 0.05. Gene sets with a maximum size of 550 and a minimum size of 20 were included in the analysis.

Electrophoresis and Western blot analysis

Samples were quantified with DC™ Protein Assay Kit II (Bio-Rad® #5000112) and the same amount of protein (40 µg) was incubated with Laemmli Loading Buffer (25% Tris-Base at 0.5 M, 0.4% SDS pH 6.8, 20% glycerol, 0.2% 2-ß-mercaptoethanol and 0.001% bromophenol blue (Merck, Germany)). Samples were boiled at 95 °C for 5 min and separated in 10% SDS-PAGE gel under reducing conditions.

Total protein staining was performed incubating the gel with Oriole (Bio-Rad® #1610496) for 90 min. The stained gels were scanned using a ChemiDoc™ Imaging System (Bio-Rad®).

For Western Blot analysis, proteins were transferred into nitrocellulose membranes (Bio-Rad® #1620115) in wet transfer at 300 mA for two hours. Membranes were blocked for 1 h at RT with SuperBlock Blocking Buffer (Thermo Fisher® #37515) and incubated overnight at 4 °C with primary antibodies. Next day, they were washed with 0.3% Tween-20 in PBS and were incubated for 1 h at room temperature with the HRP-linked secondary antibodies. SuperSignal™ West Pico PLUS Chemiluminescent Substrate kit (Thermo Fisher® #34580) was used prior to visualization in the ChemiDocTM Imaging System (Bio-Rad®). Protein bands were quantified using ImageJ® Lab software (v 4.0.1). Protein content from each sample was normalized according to total protein content.

The following primary antibodies were used for Western Blot: anti-CD9 (1:500, Invitrogen® #10626D), anti-CD81 (1:250, Santa Cruz Biotechnology Inc® #sc-166029), anti-MFGE8 (1:1500, Invitrogen ® #PA5-109955),

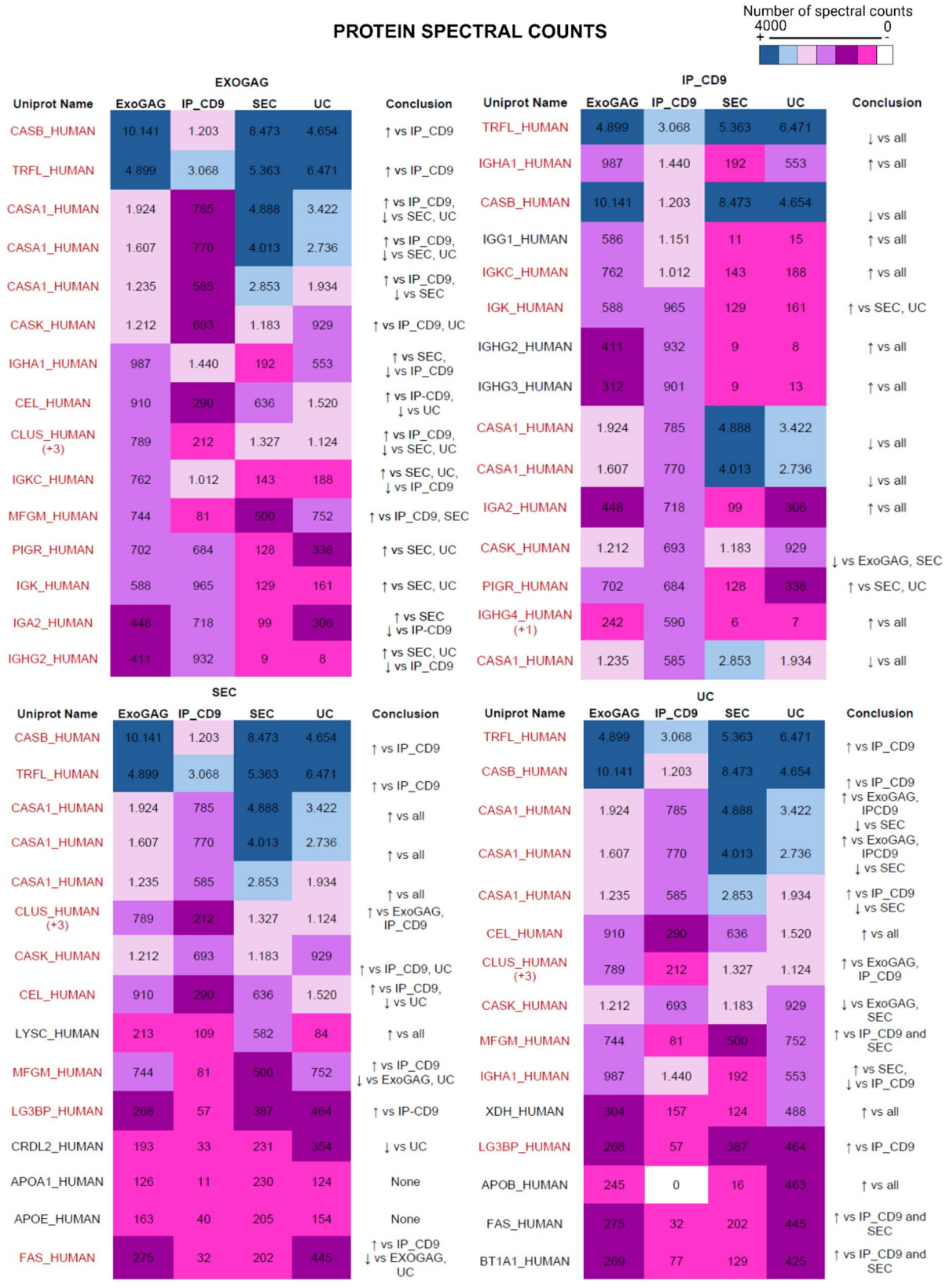

Fig. 3 (See legend on next page.)

(See figure on previous page.)

Fig. 3 Tables of TOP15 protein spectral counts detected in each isolation technique. Proteins found in ExoGAG TOP 15 are coincident to most enriched proteins in the rest of the methods, meaning that includes almost the same recovery as the other three techniques all together. Data are ordered from higher to lower spectral counts according to the color code described. Proteins found in more than one method are highlighted in dark red. The abundance of the protein in the technique is compared to its abundance in the rest of the methods in the right column of each table. ↑ means upregulated. ↓ means downregulated. None means the protein abundance is included in the same group. Colors correspond to: dark blue > 4000 counts, light blue 4000 – 2000, light pink 2000 – 1000, violet 1000 – 500, dark violet 500 – 250, pink 250-1, white 0

anti-TSG101 (1:1500, Invitrogen® #PA5-31260), anti-ALIX (1:1000, Santa Cruz Biotechnology Inc® #sc-53540) and anti- beta Casein (1:10000, Abcam # ab205301). Secondary antibodies Goat anti-Rabbit IgG HRP (1:10000, Thermo Fisher® #31460) or Goat anti-Mouse IgG HRP (1:5000, Thermo Fisher® #31430) were used when appropriated. For detailed information, please refer to Supplementary information section.

Transmission electron microscopy (TEM)

TEM was carried out in the Microscopy Service of the University of Santiago de Compostela (USC). 5 µL of the sample were spotted on carbon film-coated electron microscopy grids (Formvar, Gilder-Grids) and contrasted with a phosphotungstic acid solution. Images were acquired at 200 kV on a JEOL 2010 microscope.

Single-particle interferometric reflectance imaging sensor (SP-IRIS)

We performed the analysis in ExoView R200 (Unchained labs, USA) and Leprechaun Exosome Human Tetraspanin Kit (#NAV251-1044, Unchained labs, USA)). The protocol was followed according to the manufacturer's instructions. Chips were pre-scanned to measure the background signal. 50 µL of diluted samples (raw milk and mEVs UC 1:2000, mEVs ExoGAG 1:1000) were added to the chips and incubated overnight without shaking. Chips were washed using ExoView® CW100 plate washer and the fluorophore-labelled antibodies (CF488-anti-CD9, CF647-anti-CD63 and CF555-anti-CD81) were added. Then, chips were washed again with Washing Solution A, B and deionized water and dried at RT. Once dried, they were scanned for interferometric and fluorescence imaging. Results were analyzed with the ExoView® Software Suite, adjusting the fluorescence cutoffs individually to restrict the number of detected particles on MIgG capture spots. For detailed information, please refer to Supplementary information section.

Lipid measurements

Cholesterol and triglycerides were both measured in milk samples and mEVs isolated by UC and ExoGAG to determine its removal after isolation procedure. Concentrations were determined by standard procedures using an ADVIA-2400 Analyzer (Siemens Diagnostic Systems, Germany) in Clinical Analysis Unit from Hospital Clínico Universitario of Santiago de Compostela (CHUS).

Statistical analysis

Data are presented as mean ± SEM in all cases (bar or point plots). For deep characterization, normal distribution was confirmed by the Shapiro-Wilk test.

In case data was not normally distributed, the Kruskal-Wallis test was performed, followed by pairwise Dunn's post-hoc tests with Benjamini-Hochberg correction for multiple testing. For normally distributed data, one-way ANOVA was used for multiple comparisons. All statistical analyses and figure plotting were carried out using GraphPad Prism® Software (version 9.0) and R v4.4.0 in RStudio v2024.04.0 along with the following external packages: dplyr v1.1.4, rstatix v0.7.2, envalysis v0.7.0, ggplot2 v3.5.1 [22], ggbreak v0.1.2 [65], ggpubr v0.6.0, gt v0.11.0 and gridExtra v2. P-values less than 0.05 were considered statistically significant (*). Furthermore, ** corresponds to p-values < 0.01, *** to p-values < 0.001, and **** corresponds to p-values < 0,0001. For detailed information, please refer to Supplementary information section.

Results

Characterization of the human milk EVs fraction

Two milliliters of three different pools of milk were preprocessed in similar conditions and then EVs isolation was performed by four different methods: ExoGAG, IP_CD9, SEC and UC (Fig. 1A). Characterization of the vesicular component was initially measured by Zetasizer NanoZS to determine size and distribution of the samples (Fig. 1B). EVs distribution was similar in 3 independent measurements showing a specific profile for each isolation method. EVs sizes were the expected, ranging between 40 and 1000 nm [69]. EVs markers detected by mass spectrometry (MS) indicate that all methods met the stablished criteria required by MISEV 2023 guidelines for EVs studies [63] (Fig. 1C).

Proteomic analysis of the human milk EVs fraction

Qualitative LC-MS/MS with Data-Dependent Acquisition (DDA-MS) and quantitative SWATH-MS analysis were performed for further functional EVs characterization of all tested methods. PCA analysis reveals that more than 75% of the differences can be explained only with the first two components. All four methods are well differentiated from one another, although there is a slight overlap between UC and SEC. ExoGAG has better dataset clustering among all techniques, especially

in comparison to SEC and UC, which are more dispersed (Fig. 2A). In addition, DDA-MS analysis indicates that ExoGAG also recovers more total count, as well as specific peptides and proteins detected by the method (Fig. 2B-C) with statistical significance (Supplementary Fig. 3A-B). Interestingly, the vast majority of the detected proteins are shared between ExoGAG and UC (≈75%, Fig. 1D), whereas IP_CD9 has poor recovery among all methods. Comparing the results with Vesiclepedia database [9], we can see that ExoGAG isolates more EVs proteins than the rest of the techniques. In addition, we observe that ExoGAG recovers more specific EVs proteins ($n = 30$; 6,6% of recovered proteins) than UC ($n = 12$; 6%), IP_CD9 ($n = 2$; 1%) and SEC ($n = 0$; 0%), respectively (Fig. 1C). Further analysis by SWATH-MS indicates all methods have comparable recovery, with ExoGAG and UC being the most similar in isolating total and EVs protein (Supplementary Fig. 3 C).

Selecting the TOP 15 proteins identified by each technique in the DDA-MS we observed differences in recovery and abundance (Fig. 3). Interestingly, all TOP 15 proteins found in ExoGAG are coincidental to most enriched proteins in the rest of the methods. Also, all four methods heavily isolate different types of caseins, which are considered contaminants in milk EVs preparations. In addition, the same analysis of TOP10 proteins using areas under the curve (AUC) obtained with SWATH-MS analysis, showed similar recovery between techniques except for IP_CD9, which had a minority of shared proteins with the other methods (Supplementary Fig. 4).

The DDA-MS analyses indicate that the proteins identified by the different techniques are related to similar biological processes (Fig. 4), with the immune system, metabolism and cellular processes being more represented. Also, the main enriched terms correspond to these three biological processes, especially the immune system, with neutrophil degranulation and humoral response being highlighted. Although the functional profiles among all techniques are similar, the p-values increase with ExoGAG and UC. SWATH-MS analyses of molecular function, biological processes involved and enriched terms are similar to those of the DDA-MS results (Supplementary Fig. 5). However, protein metabolism and signal transduction become more relevant biological processes than those observed by DDA-MS (Supplementary Fig. 5B), as well as extracellular matrix organization and neutrophil degranulation are the mostly observed related enriched terms (Supplementary Fig. 5 C).

Then, we carried out the protein interaction analysis for DDA-MS proteins recovered in the four methods (Supplementary Fig. 6). There are some constant clusters corresponding to the same family of proteins, similar functions and similar location in the cell. Standing out among the different locations we can see ribosome proteins in green, cytoplasmic proteins in dark and light red and nuclear in light blue. Also, the are some conserved family proteins between methods such as family of proteins which mediate signal transduction by binding to phosphoserine-containing proteins in yellow and keratins in light pink. Regarding function, the three proteins in grey common between the four groups seem to be involved in the milk fat globule (MFG) interactions with the cytoplasmatic membrane. Surprisingly, in all the analyzed methods except for IP_CD9, we can find the family protein of chromatin-modifying protein/charged multivesicular body protein family.

However, this similarity does not hold when analyzing the SWATH-MS data (Fig. 5). Apart from ribosomal and cytoplasmic proteins, hardly any protein groups or families are found in common between the comparisons between techniques.

In addition we compared the DDA-MS data with those from SWATH-MS in order to give more accuracy to our study, we also wanted to contrast the results from FunRich and Metascape with those from the Reactome Pathway Database (Fig. 6). First, we selected the groups with the highest number of proteins involved. We then checked the common biological processes associated with the proteins that were differentially expressed in ExoGAG vs. all the techniques individually. Once again, we found the immune system (Fig. 6A) and protein metabolism (Fig. 6B) as the most important processes, this time also accompanied by the metabolism pathway (Fig. 6D). The results again correspond to those found with SWATH-MS, adding only the developmental biology pathway (Fig. 6C) to those mentioned above.

Glycomics of the human milk EVs fraction

We also characterized the glycosignature of each method after isolating and characterizing milk EVs in relation to their protein and peptide components (Fig. 7). To do so, we initially selected only EVs proteins according to the Vesiclepedia database. ExoGAG was the most efficient method isolating total EVs proteins and peptides, although there were only statistically significant differences compared to raw milk (Fig. 7A.1 and 7B.1). Regarding the glycosylated fraction, once again, the best performance for glycoproteins was obtained by ExoGAG, being statistically significant with respect to IP_CD9 and raw milk (Fig. 7A.2). However, for glycopeptides, UC was the technique that stood out, although no statistical differences were observed between techniques (Fig. 7B.2). Interestingly, for both measurements, the ExoGAG samples showed a lower scattering index (Fig. 7A.2-B.2).

The main part of the glycated proteins in milk are N-glycans [62]. Among them, we find four main subgroups: fucosylated, fucosiallylated, sialylated and

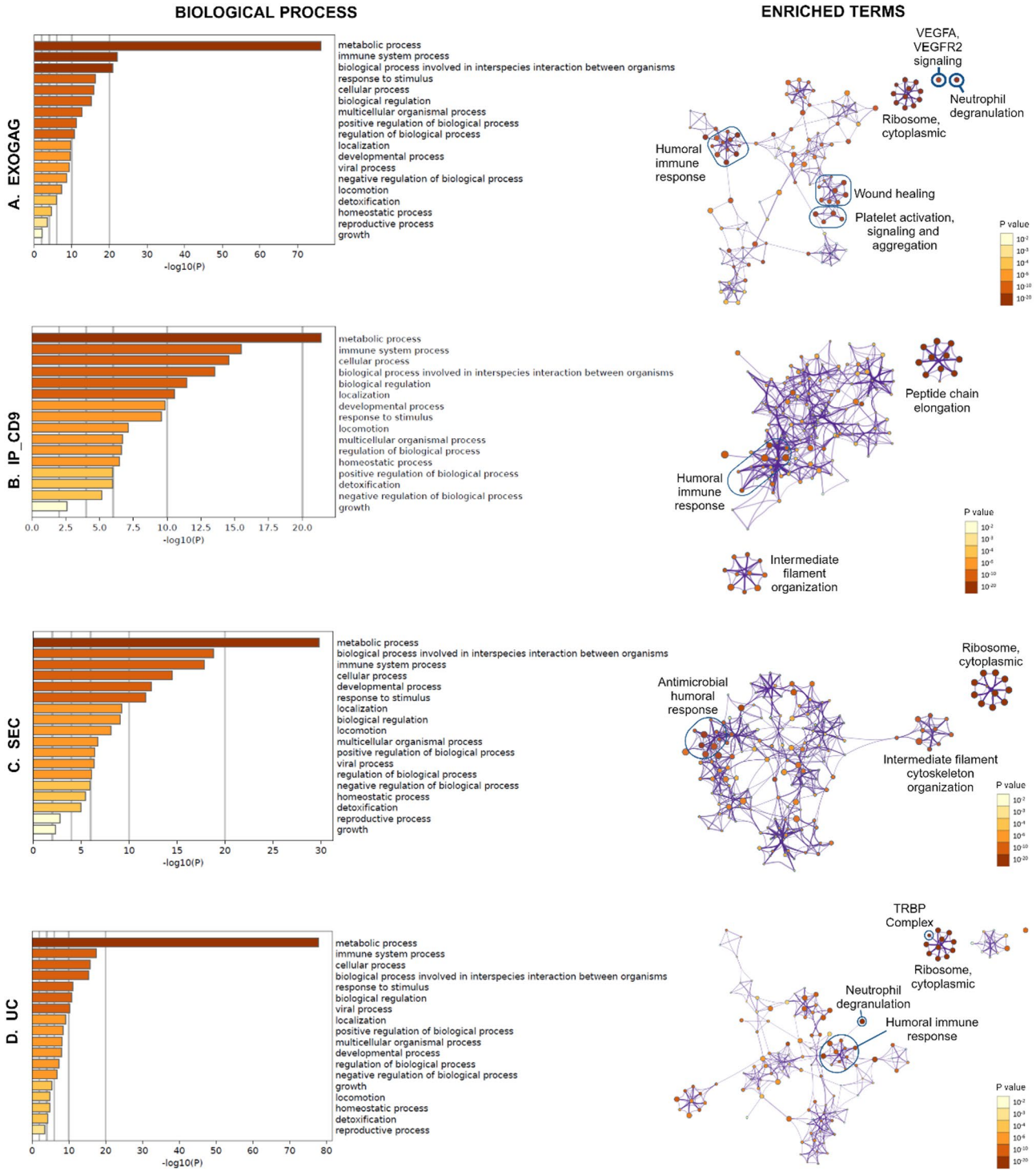

Fig. 4 Functional analysis of biological processes and enriched terms of DDA-MS data with Metascape tool. Both biological processes and enriched terms of proteins found in DDA-MS analysis after isolation with (**A**) ExoGAG, (**B**) IP_CD9, (**C**) SEC and (**D**) UC were described. All methods showed coincidental biological processes although specific terms were more variable

oligomannose. The rest and the O-glycans are grouped in the "others" category. As we can see, depending on the isolation method we obtain different glycosignatures that can be more or less related to that of raw milk (Fig. 7A.3 and 7B.3). If we compare the N-glycoproteins (Fig. 7A.3) we can see that IP_CD9 completely lacks one of the subpopulations, fucosialylated proteins. These are preferably kept after isolation with ExoGAG and SEC, although they

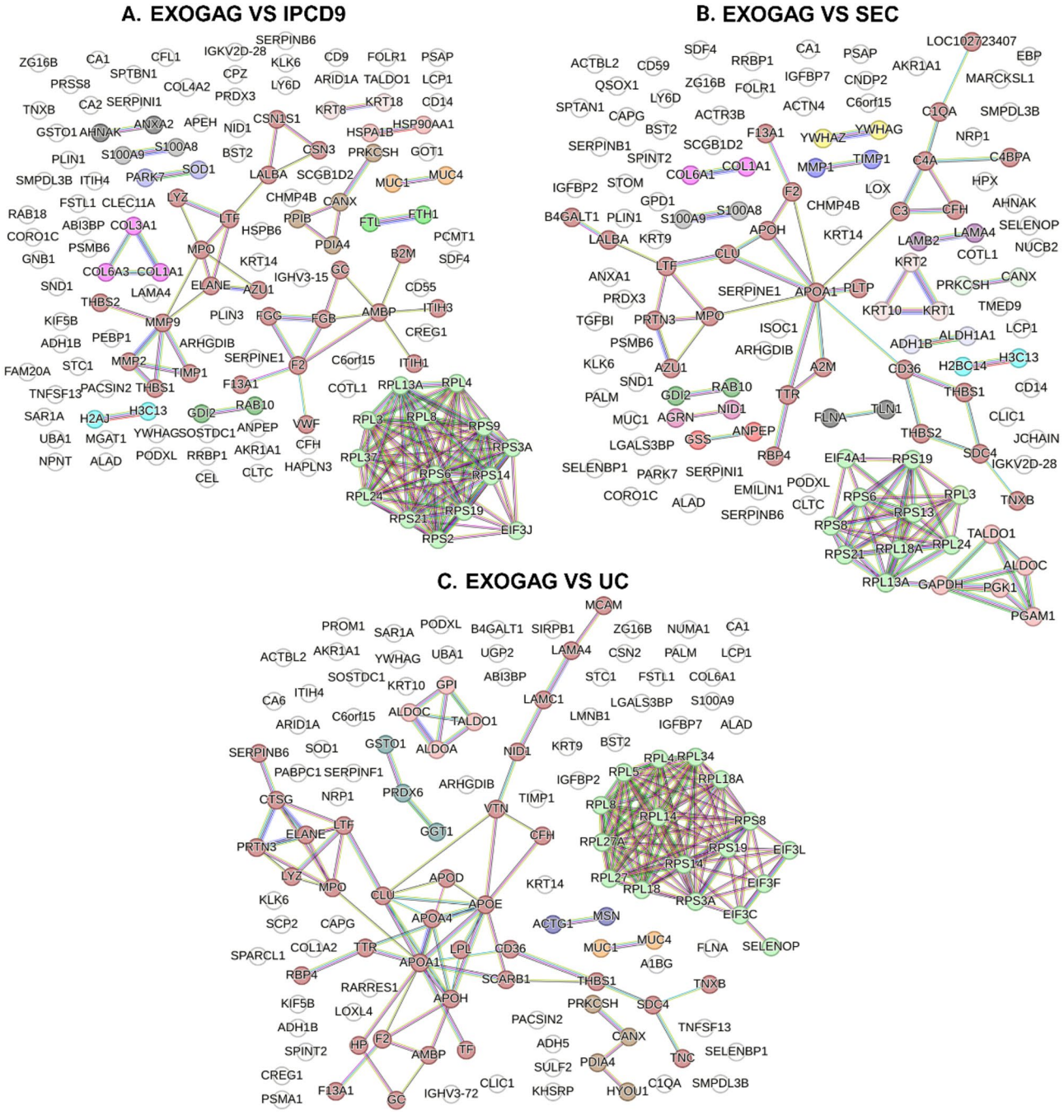

Fig. 5 Interactions between proteins found in the SWATH-MS analysis after isolation with the four methods. Comparisons between proteins yielded in (**A**) ExoGAG vs. IP_CD9, (**B**) ExoGAG vs. SEC and (**C**) ExoGAG vs. UC were performed. The main part of the clusters are only represented in each one of the comparisons, except for the ribosomal cluster in light green and cytoplasmatic proteins in dark red

are also detected by UC but in a lower proportion. It is common for all methods that fucosylated, sialylated and oligomannose proteins comprise approximately 20% of the total N-glycans, except in UC which seems to preferentially isolate fucosylated proteins.

Regarding N-glycopeptides, the proportions vary both in raw milk and after EVs isolation (Fig. 7B.3). In this case, we find again that IP_CD9 lacks fucosialylated peptides, although it enriches the sialylated ones, which are a minor population in raw milk. Unlike IP_CD9, the predominant subpopulation in the other methods is fucosylated peptides (similarly as in raw milk), followed by sialylated and oligomannoses. Although fucosylated peptides remain the smallest subpopulation, ExoGAG and SEC are the techniques that adequately maintain this group.

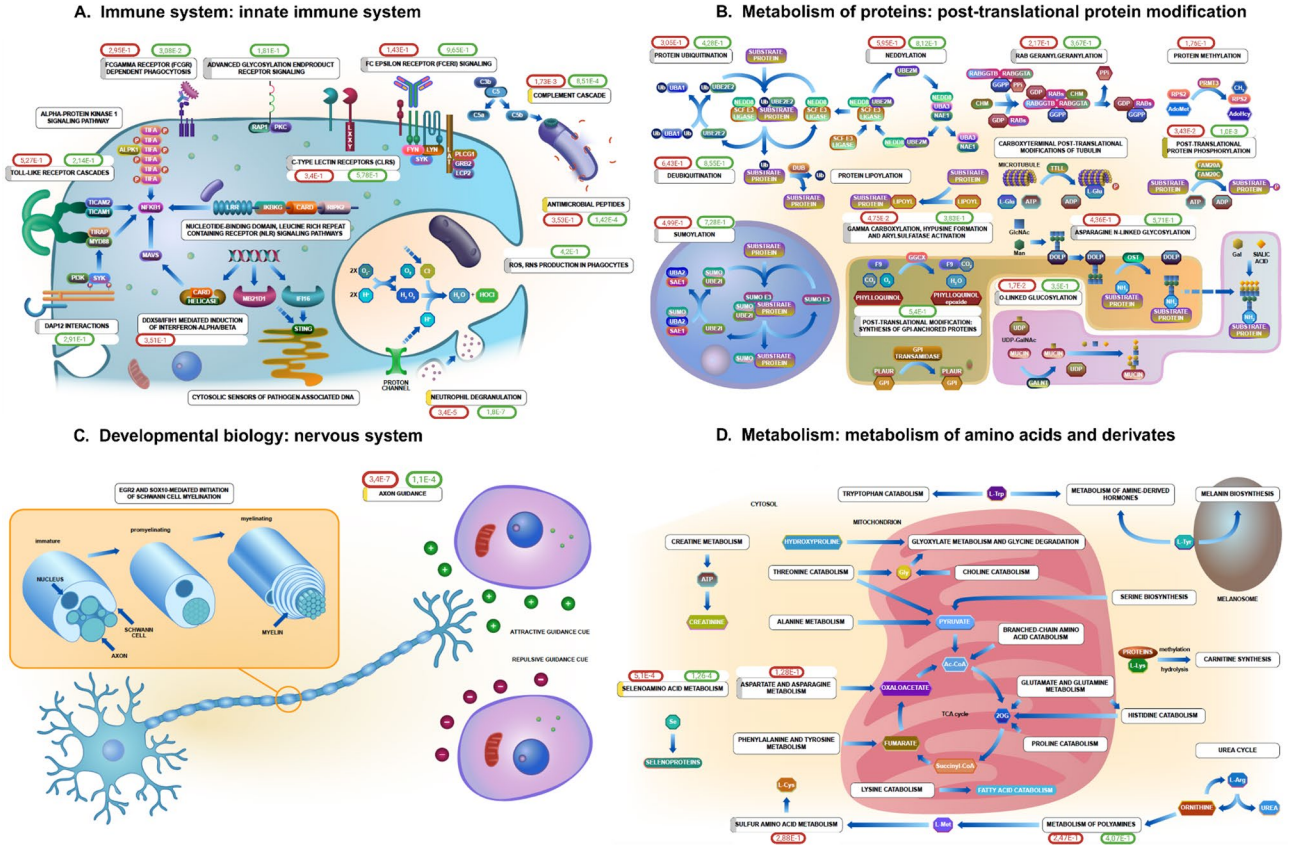

Fig. 6 Functional analysis of DEPs detected by SWATH-MS after the EVs isolation techniques analyzed with Reactome. Analysis of DEPs revealed that (**A**) immune system, (**B**) protein metabolism, (**C**) developmental biology, and (**D**) metabolism are central processes to which human milk may be contributing during infant growth. Among these identified biological processes the immune system is mainly represented by the innate immune system being neutrophil degranulation, the complement cascade and the antimicrobial effect detected with lower FDRs than the rest of the paths. Metabolism of proteins seems to be highly affected by post-translational modifications, outstanding phosphorylation among the others. Similarly, the nervous system appears as central in developmental biology processes, with a key role in axon guidance. Finally, metabolism of amino acids and derivates stands out from the pathways includes in metabolism, gaining higher importance the metabolism of selenoamino acids. FDR was calculated as the average of FDRs for each pool of milk for the exact same process for its up and down regulated proteins in ExoGAG vs. the other three techniques individually. Red circles belong to upregulation; green circles belong to downregulation

Transcriptomic analysis of human milk EVs

In order to determine the optimal procedure to isolate EVs from milk to perform transcriptomic studies on the same samples used for the proteomic study, we also compared the same four different isolation methods (UC, SEC and IP_CD9, ExoGAG) analyzing their total RNA recovery potential and miRNA expression profiles. UC and ExoGAG achieved very high total RNA concentrations with much better yield (Fig. 8A) and purity (Fig. 8B) than SEC and IP_CD9. For both purity ratios (A260/280 and A260/230) UC and ExoGAG met the minimum quality standards [16], while IP_CD9 and SEC had lower values.

We also determined miRNA expression profiles using the nCounter® Human v3 miRNA Assay CSO Panel (Nanostring) that includes a panel of 827 biologically relevant miRNAs (Fig. 8C) to compare the number of miRNAs detected between the different techniques. The highest number of miRNAs with less dispersion was obtained with ExoGAG, being similar to those of UC but with lower sensitivity in each of the counting ranges, even in the most rigorous one (> 100 counts). SEC and IP_CD9 resulted in insufficient performance and quality values.

Then, we carried out a Gene Ontology (GO) analysis selecting those miRNAs > 100 counts which overlapped between the three pools isolated by each of the four methods (Fig. 8D). SEC samples were not suitable for the analysis as no miRNAs were common between the three pools isolated with the method. IP_CD9 analysis detected only two miRNAs (Supplementary Fig. 7) with an extremely low gene ratio. In contrast, ExoGAG (Fig. 8D.1) and UC (Fig. 8D.2) analysis were more sensitive, finding 15 and 10 deregulated miRNAs with lower adjusted p-values and higher gene ratios. In addition, ExoGAG detected almost the same miRNAs as UC except for two of them (miR-30b-5p and miR-499a-5p)

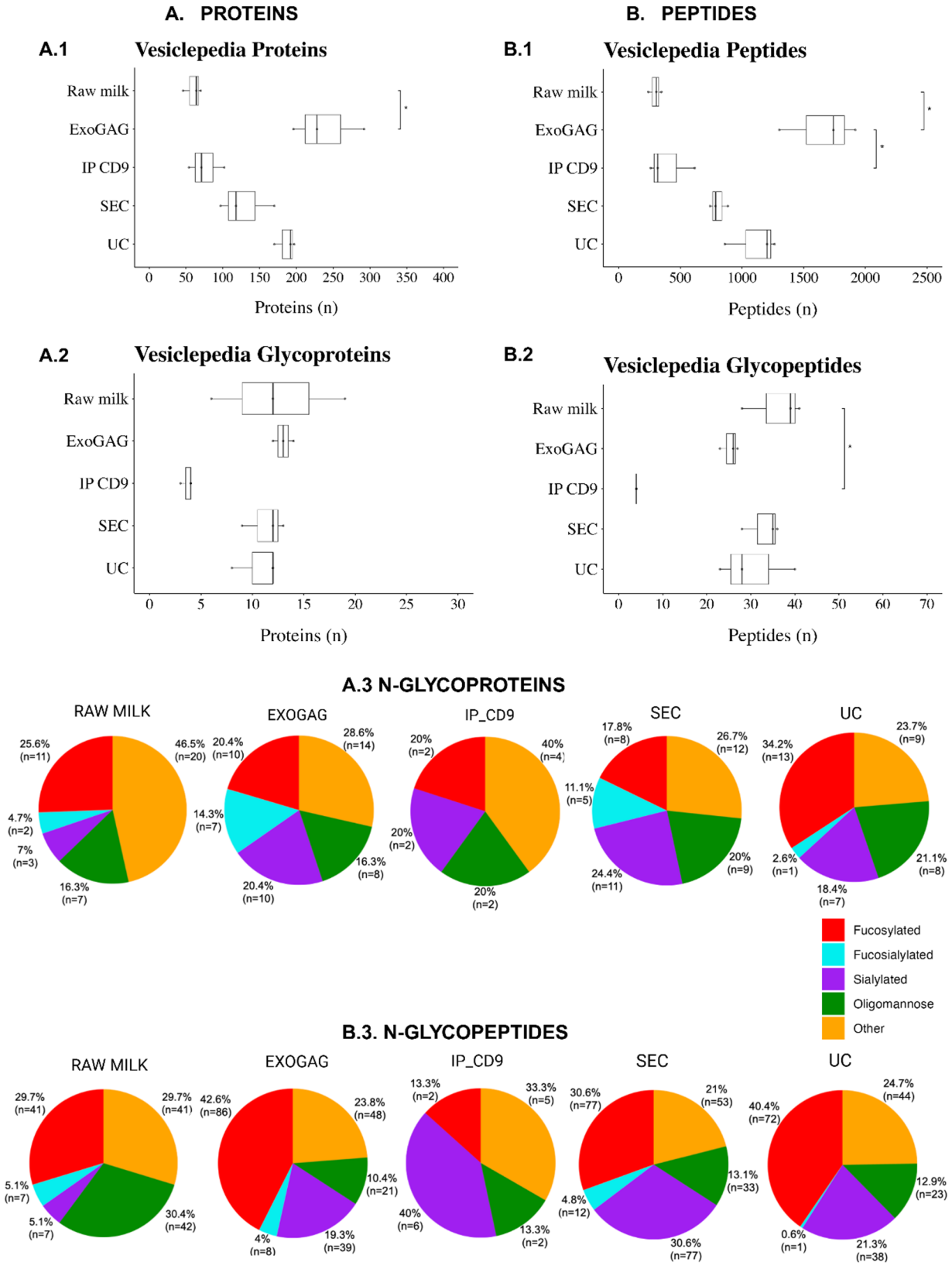

Fig. 7 (See legend on next page.)

(See figure on previous page.)

Fig. 7 Glycomic analysis of the vesicle-related fraction of raw milk and after isolation with ExoGAG, IP_CD9, SEC and UC. (**A**) Protein and (**B**) peptide recovery before and after the isolation with the four methods. We first selected only vesicle-related (**A**.1) proteins and (**B**.1) peptides and then compared only the glycated fraction of both (**A**.2) proteins and (**B**.2) peptides. Sectors diagram of (**A**.3) glycoproteins and (**B**.3) glycopeptides detected by each technique. Bars represent means ± SEM. Kruskal-Wallis omnibus test and pairwise Dunn's post-hoc tests applying Benjamini-Hochberg correction was used. $p < 0.05$ was considered significant. Only significative comparisons are shown: * $p < 0.05$

while identified seven (miR-15a-5p, miR-15b-5p, miR181a-5p, miR-200c-3p, miR-21-5p, miR-29c-3p and miR-30e-5p) unique miRNAs. In conclusion, ExoGAG and UC were the most suitable techniques for miRNA analysis and proteomic studies in the same samples.

Deeper extracellular vesicle characterization following MISEV guidelines

Since UC and ExoGAG have proven to be the most efficient techniques for proteomic and transcriptomic studies of breast milk EVs isolated in the same samples, the vesicular profile was further studied through the identification of possible differences between both methods based on contaminants carried over and EVs markers, shape, size and composition of the vesicles extracted by both methods.

Lipid profile of Raw milk and mEVs

Milk contains colloidal structures such as casein micelles (100–200 nm) and fat globules (0.1–15 μm) that match in size and density with EVs, making its analysis difficult ([42, 43, 53]. The lipid core of milk fat globules (MFG) is made up of neutral lipids (such as cholesterol) or triglycerides, characteristics that differentiate them from mEVs [3].

Therefore, we measured triglycerides and cholesterol to check the level of contaminant removal after mEVs isolation compared to raw milk (Supplementary Fig. 8). Both techniques are able to remove almost all triglycerides and a large part of cholesterol (Supplementary Fig. 8 A), with ExoGAG being 20% more efficient than UC (Supplementary Fig. 8B).

EVs markers

Total protein stain shows a constant fingerprint between the three pools in raw milk and after mEVs isolation with both techniques, with small variations in the intensity of the bands (Fig. 9A). Next, we detected five of the EVs markers included in three of the categories established by the MISEV2023 guideline [63]: (1) CD9 and CD81 as transmembrane or GPI-anchored proteins associated with the plasma membrane and/or endosomes (category 1, Fig. 9B), (2) ALIX and TSG101 which are included in the cytosolic proteins recovered in EVs (category 2, Fig. 9C) and (3) MFGE8 (milk fat globule epidermal growth factor 8) also known as lactadherin and considered as a secreted protein recovered with EVs (category 5, Fig. 9D). In addition, the presence of β-casein (Category 3, NVEPs) was also studied, observing a significant decrease in both techniques compared to raw milk. In contrast, TGBFI was only properly detected in raw milk and in UC mEVs, being hardly detected in ExoGAG mEVs, indicating the absence of interferers after their isolation (Fig. 9E). In general, both techniques preserve the required markers for the characterization of milk EVs, although after normalizing their detection based on total protein, it is observed a tendance for ExoGAG to recover the markers better than UC, except for CD81, with no significant differences between both while lacking vesicular contaminants.

Single-vesicle characterization

MISEV2023 guidelines suggest the characterization of individual vesicles by two different but complementary techniques. We used TEM for high-resolution imaging of EVs shape and size (Fig. 10A). Interestingly, TEM highlights the isolation method, densely labelling two types of vesicular populations. On one hand, vesicles that range from 50 to 200 nm contained in the ExoGAG-GAG-Vesicle complex due to the aggregation method (precipitated). On the other hand, vesicles of approximately ~ 200 nm in size that are not part of the ExoGAG-GAG-Vesicle complex (Free). Furthermore, we characterized EVs subpopulations using SP-IRIS technology, based on tetraspanin interferometry and immunofluorescence labelling (Fig. 10B). We developed an analysis of tetraspanin subpopulation proportion and abundance (CD63, CD81 and CD9, Fig. 10C) and total EVs concentration in raw milk and mEVs isolated by ExoGAG and UC (Fig. 10D). It is observed that the tetraspanin subpopulation profiles of ExoGAG and UC were almost identical, where CD81 was the main component, followed by CD63 and CD9 respectively. Regarding total vesicle count, a higher concentration of mEVs isolated by UC was obtained, although both remained in the same order of magnitude (Fig. 10D).

Discussion

Currently, studies involving extracellular vesicles had increased enormously promoting an urge to set some specific requirements to accept conclusions on the involvement of EVs, which are included in MISEV2023 guidelines [63]. Thus, we have followed those recommendations for the experimental design of all the experiments included in the manuscript.

For this study, we started by establishing a group of centrifugation steps prior to EVs isolation so as to remove interferers that could influence the outcome of the experiments. On top of that, we optimized the volume required for mEVs isolation by UC, so that all the experiments could be developed. In previously published literature, UC required at least 25 mL [3, 29, 45], which is an extremely high amount of milk considering the experimental design of this study, where we perform various omics analysis and a deep characterization of the vesicular fraction. We managed to decrease the required volume from more than 25 mL down to 2 mL, making the method comparison possible.

In research, reliability (precision, consistency and reproducibility) corresponds to a psychometric property characterized by the lack of measurement error, or the degree of consistency and stability of the values obtained throughout successive measurements with the same method [41]. For this reason, we have used the same EVs isolation methods on the same samples used for proteomic, transcriptomic and glycomic studies, so that we could compare conclusions obtained from the results and interpretation of both approaches.

After the mEVs isolation by the four methods, we could conclude that all of them were successful as the characterization showed the appropriate sizes and EVs-related markers confirming vesicular entities were enriched after the isolation, although there is a better marker yield detection by ExoGAG and UC, in comparison to SEC and IP_CD9 (Fig. 1).

The rapid innovations of omics technologies have revolutionized the field of biomedical research, enabling the profiling of various biological layers such as the genome, epigenome, transcriptome, proteome, and metabolome. These technologies generate vast amounts of data, which, when integrated, provide a comprehensive understanding of biological systems and their interactions gaining a holistic understanding of biological systems [19, 12]. In consequence, we have performed for the first time a study integrating mEVs proteomics, transcriptomics and glycomics achieving a deeper and more comprehensive view of their implications and improving the predictive value of our findings.

The proteomic analyses showed that ExoGAG stands out as the technique with improved performance among the four. The PCA suggests that EVs studies with ExoGAG tend to be more uniform and reproducible than those obtained by the other standard techniques in equal conditions, as the samples are clustered without overlapping with other techniques and with low dispersion. Furthermore, both protein and peptide abundance were higher in comparison with the other techniques, and similarly, this was also true for vesicle-related proteins and peptides (Fig. 2).

It has been shown that recovery and abundance of proteins are technique dependent [11, 71]. We confirmed that as the abundance of the spectral counts identified by DDA-MS, ExoGAG seems likely to include the same recovery as all of the other techniques all together, as TOP15 proteins present in ExoGAG were coincident with those isolated by all the other methods (common proteins in red, Fig. 3). Furthermore, we also obtained an elevated concentration of caseins, which are considered contaminants, indicating the need for further purification steps in case of functional studies being performed to ensure purity [3, 63]. If we had included a precipitation step prior to EVs isolation with EDTA or via acidification as MISEV2023 suggests, we could have potentially been able to remove the contaminants from the final sample but we would also have been likely to eliminate a lot of valuable information from our samples, as depletion steps are not specific to only the target protein, eliminating as well some relevant others from the sample. Furthermore, although depletion is recommended in MISEV there is no standard protocol to this methodology and published literature shows different procedures depending on the author. In this scenario, we have prioritized recovery among all for omics studies, as we can after process our data taking only into account EVs proteins. Even though we cannot ensure a complete lack of interference with our approach we sustain that this was the best option considering our final goal and the possibilities that the omics analysis gave us to overcome this issue.

Furthermore, DDA-MS interaction between proteins analysis detected a group of common clusters between techniques, such as ribosomal or nuclear. However, in all the analyzed methods except for IP_CD9, we can find the family protein of chromatin-modifying protein/charged multivesicular body protein family which is involved in degradation of surface receptor proteins and formation of endocytic multivesicular bodies (MVBs) in dark pink. These MVBs are involved in the biogenesis of exosomes, as once they bind to the cytoplasmatic membrane they shed them into the extracellular space. This finding suggests a lower capacity of IP_CD9 technique to properly isolate the vesicular fraction in comparison to the other methods (Supplementary Fig. 5). In contrast, SWATH-MS interaction analysis showed that mainly all the clusters found are different, except for the ribosomal proteins, meaning that all the represented proteins are detected by ExoGAG while the rest of the methods only identified some of the common ones. This statement again supports the idea that ExoGAG robustly encompasses the recovery of all the other techniques together (Fig. 5).

We have identified by different techniques and tools several important proteins related to the immune system and metabolism (Fig. 6A-B). Immune-related proteins

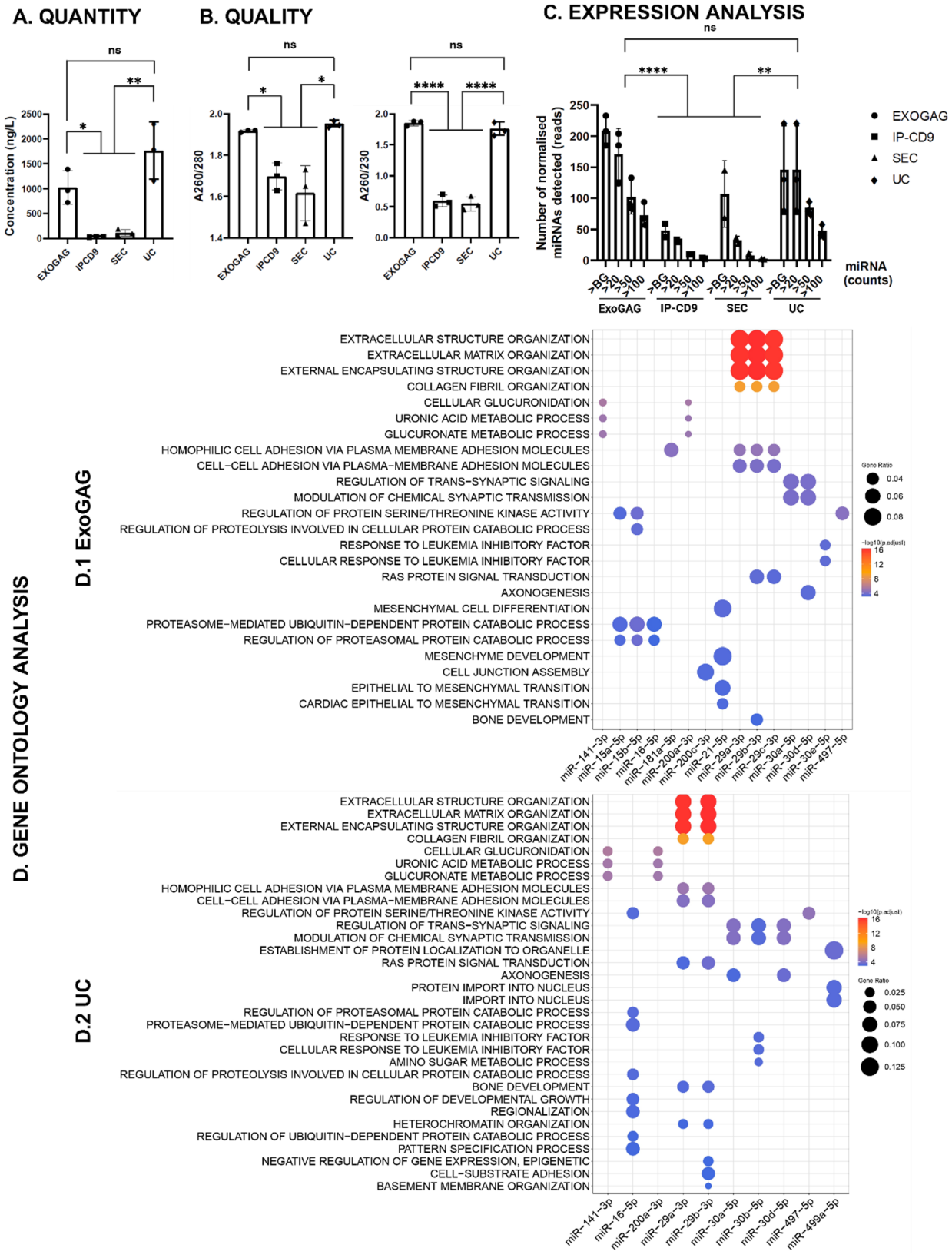

Fig. 8 (See legend on next page.)

(See figure on previous page.)

Fig. 8 RNA extraction, miRNA expression and Gene Ontology (GO) analysis of mEVs isolated by ExoGAG, IP-CD9, SEC and UC. (**A**) Quantity of miRNAs detected after milk EVs isolation by the four techniques. The quality of the miRNAs obtained was determined by measurements in Agilent 2100 Bioanalyzer considering (**B**) A260/280 ratio and A260/230 ratio. (**C**) Expression levels detected after performing nCounter® Human v3 miRNA Assay CSO Panel Assay to mVEs isolated by ExoGAG, IP_CD9, SEC and UC. (**D**) Bubble plot showing the statistically significant terms from GO database, grouped by miRNAs > 100 counts common for pools isolated with the same method. Concentration and quality criteria were met after ExoGAG and UC isolation with high levels of statistical significance. miRNA expression was significantly enhanced with ExoGAG and UC compared to the other techniques, although the first presented higher values and less dispersion in every category. It should be noted that the number of miRNAs detected > 100 counts, representing the detection of the highest expressed miRNAs, constitutes the most robust and valuable result. The average detection in this category was 72 and 43 counts in ExoGAG and UC respectively. Furthermore, GO analysis showed a good recovery for UC and ExoGAG, improving the detection with the last. One of the samples from the SEC and IP_CD9 groups had to be removed due to poor quality derived from the extraction. RNA extraction was developed twice to avoid technical bias. Values close to 2.0 means RNA purity for A260/280. Values between 1.8 and 2.2 means RNA purity for A260/230 ratio. The size of each point in bubble plots is proportional to the gene ratio, defined as the number of genes in the input list annotated to the corresponding term divided by the total number of genes in the input list. The color of the points represents the $-\log_{10}$ adjusted P-value from the enrichment analysis. Two-way ANOVA with multiple comparisons was used and a value of $p < 0.05$ was considered significant. ns represents not significative, * $p < 0.05$, ** $p < 0.01$, *** $p < 0.001$, **** $p < 0.0001$

are directly involved in neutrophil degranulation, the complement cascade and the antimicrobial effect, all of which are directly involved in the innate immune system. These results confirm that mEVs have implications in the infant with its first form of immunity by containing a large amount of proteins involved in the defense against external organisms and which will contribute to the proper functioning and development of its immune systeorm of immunity by containing a largeamount of proteins involved in the defense against external organisms and wm, in agreement with what has been previously described in the literature [21, 57, 60, 72]. In addition, the proteins identified also show great involvement in protein metabolism. Post-translational modifications are responsible for the regulation of proteins through their structure, localization function and activity [32, 67, 69, 70]. Phosphorylation stands out above the rest of the processes in our analysis. Phosphorylated peptides have been described to be instrumental in increasing the bioavailability of essential minerals involved in multiple physiological processes, containing antioxidant and anti-inflammatory properties [55]. This implies that milk is a nutritional source par excellence, providing the necessary requirements for newborns.

Interestingly, we observed that developmental biology and metabolism pathways are also one of the main components of human milk EVs. The developmental biology process is the main category involved in the development of the nervous system (Fig. 6C), responsible for the correct neuronal structuring and synaptic connections that determine brain chemistry in adulthood [61]. This role is mediated by oligosaccharides present in milk, which have been described to mediate several neuronal processes such as axon guidance [33]. In our analysis, axon guidance is found to have very low FDR values, supporting previously published results and consolidating the fact that mEVs, especially glycosylated proteins contained on them, might play a crucial role in neurodevelopment. Metabolism is also dysregulated both up and down, but it is more represented in downregulated proteins (Fig. 6D). Finally, another identified mechanism is the metabolic pathway of amino acids and derivatives, highlighting the metabolism of selenoamino acids, regulators of the function of effector and regulatory T cells and, therefore, influencing the correct functioning of immune cells [36]. Amino acids are essential for the correct preimplantation and development of the foetus and, although their function in the fully formed organism has not yet been described, it is postulated that both essential and non-essential amino acids could be beneficial for development [58]. All this data supports our previous findings where immune system and developmental biology pathways are central processes to which human milk EVs may be contributing during infant growth [48], and identify as relevant new pathways, protein metabolism and metabolism.

Regarding glycopatterns found, we could identify that ExoGAG maintains fucosialylated proteins (lost with IP_CD9) and also enriches the fucosylated fraction (highly recovered with UC), while keeping all the other subgroups. Thus, we could obtain a pattern more similar to that of raw milk than with the other methods, even though there is a clear loss of the subgroup of others. This would probably be a consequence of a greater enrichment of O-glycans in raw milk, while EVs are mainly N-glycated. In contrast, glycopeptides included in others have a more constant proportion before and after the isolation and fucosialylated peptides behave the same way as proteins. In this case, the main variations are shown in oligomannoses, whose proportion is decreased after the isolation with all the methods compared to raw milk but have a similar abundance between techniques. All in all, ExoGAG seems to provide a glycopattern that results from the combination of that found in SEC and UC, maintaining both the fucosialylated and fucosylated subpopulations and that behaves more closely to raw milk (Fig. 7).

Furthermore, GO analysis of enriched terms (Fig. 8D) showed that ExoGAG detected a higher miRNA count which included almost the same recovery as UC but including seven additional miRNAs. Strikingly among

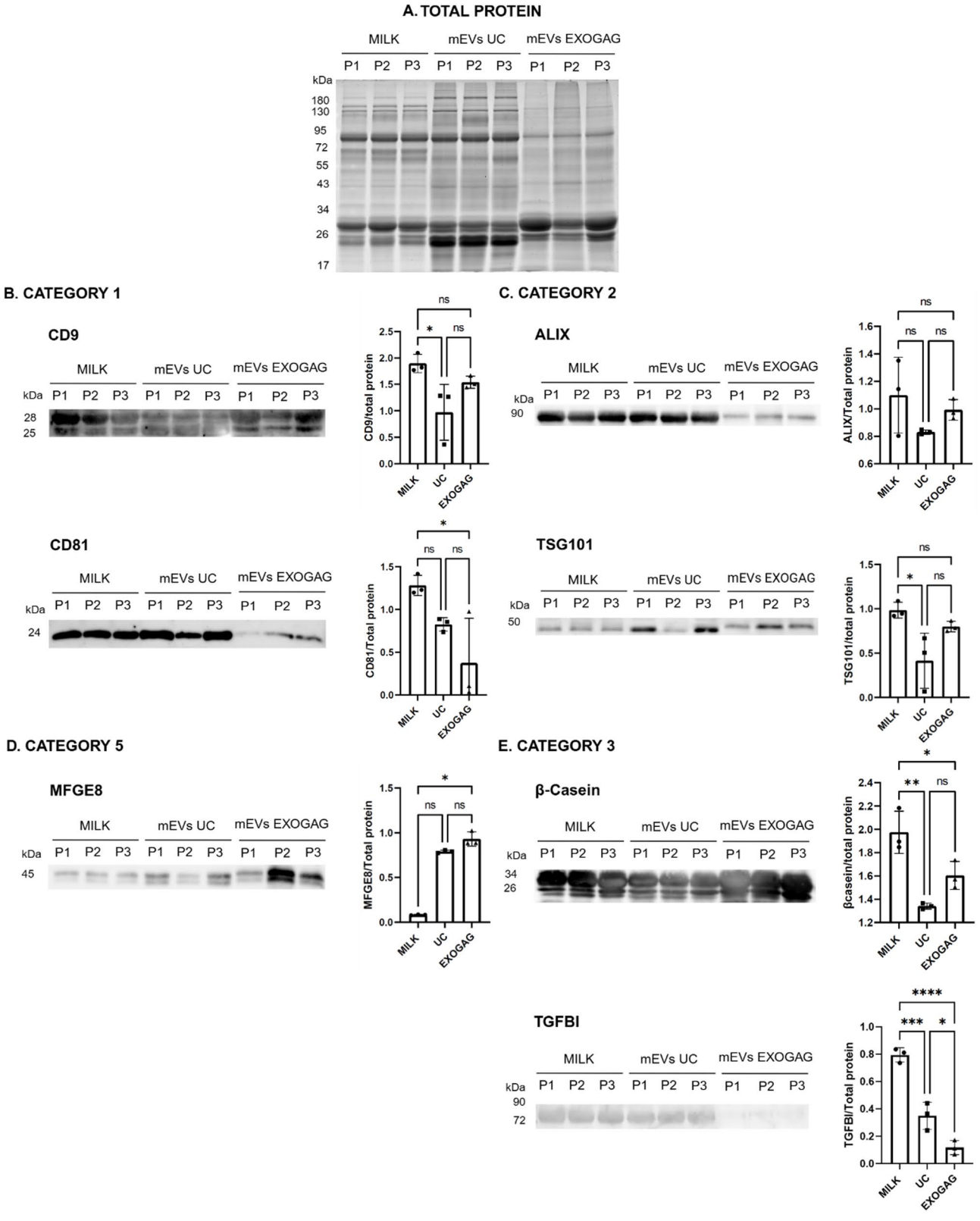

Fig. 9 (See legend on next page.)

(See figure on previous page.)

Fig. 9 Total protein and vesicle-related markers in raw milk and mEVs isolated by Ultracentrifugation and ExoGAG. (**A**) Protein fingerprint in raw milk (MILK), extracellular vesicles isolated by Ultracentrifugation (mEVs UC) and extracellular vesicles isolated by ExoGAG (mEVs ExoGAG) stained with Oriole (BioRad®). The protein abundance of the markers under the three conditions was determined by Western Blot. Furthermore, the densitometry analysis was performed for each of them making use of ImageJ. The detected EVs markers included; (**B**) Category 1: CD9 and CD81, (**C**) Category 2: ALIX and TSG101, (**D**) Category 5: MFGE8, (**E**) Category 3: βcasein and TGFBI. All markers were detected at least twice in independent experiments. P1, P2 and P3 means POOL1, POOL2 and POOL3 respectively. Total protein stain was used as a housekeeping. Ordinary One-way ANOVA with multiple comparisons was used and a value of $p < 0.05$ was considered significant: ns represents not significative, * $p < 0.05$, ** $p < 0.01$

them was miR-29c-3p, which forms part of the family of proteins found with higher significance in both techniques and whose role is associated to fibrosis suppression as well as glucose metabolism [15], both molecular processes included in metabolic pathways. Similarly, as we saw in the proteomic data, the principal enriched terms are associated with metabolism at a high extent (extracellular matrix organization), developmental biology (regulation of trans-synaptic signaling and axonogenesis), protein metabolism (post-translational modifications and protein catabolism) as well as immune response (cellular responses to external agents). All in all, this data supports the previously identified biological processes and its specific enriched pathways as central in human mEVs, highlighting its main target roles in the infant.

As recently described by [48] after isolation of EVs from human milk and colostrum with ExoGAG in both preterm and terms mothers, gene ontology analysis unmasked a correlation between upregulated miRNAs and their implications in the infant growth and development. This finding supports the previously described pathways found in the proteomic functional analysis, where human milk is stated as the ultimate nutritional and developmental source for the newborn.

In light of the previous results, we determined that ExoGAG and UC were the best techniques to develop omics studies in the same samples. It should be noted that IP_CD9, has a limited detection power as it is only isolating CD9 positive vesicles, recovering only a subpopulation among the EVs contained in the sample, which could explain its poor performance.

When analyzing contaminants present in the EVs preparations, which are structures of similar size and density as EVs such as cholesterol and triglycerides, we concluded that almost all the triglycerides were removed, and more than half of the cholesterol as well was depleted after the initial centrifugation steps (Supplementary Fig. 7). The fact that cholesterol is not completely removed can be explained as it is a structural component of biological membranes, so these values are also related to high purity in EVs isolation.

Furthermore, we identified a group of EVs markers classified according to MISEV2023; CD9 and CD81 (category 1), ALIX and TSG101 (category 2) and MFGE8 (category 5) (Fig. 9). MFGE8 or lactadherin is a tissue-specific protein highly expressed in lactating mammary glands and secreted in association with milk fat globules (MFG). Therefore, its presence on the surface of mEVs supports their presence in the mammary epithelium, since MFGE8 is enriched in milk-producing cells [46]. Furthermore, TGFBI (category 3) absence in ExoGAG mEVs confirmed that NVEPs are removed from the EVs fraction, despite being detected both in raw milk and UC mEVs.

Finally, single-vesicle characterization included the acquisition of TEM images of vesicles isolated by both techniques, confirming their adequate size and form. It should be noted as well, the limited power of Zetasizer technology, which may seem controversial to the size found by TEM and by SP-IRIS. In consequence of Zetasizer being unable to identify individual vesicles the range is overestimated. In this case, bigger sizes detected by ExoGAG method showed the expected GAGs and EVs aggregation complex, as the method creates a big entrapment of vesicles as shown in TEM images in Fig. 10A. Moreover, SP-IRIS let us identify that there is no bias in the tetraspanin subpopulation profile after isolation either by ExoGAG and UC, as both profiles are almost identical (Fig. 10C). Surprisingly, total EVs concentrations were higher in UC in comparison to ExoGAG, although both were highly enriched (Fig. 10D). Previously, we saw that proteins and peptides validated by Vesiclepedia were enriched after isolation with ExoGAG and the same occurred for glycoproteins. These differences in the recovery between techniques can be explained as with SP-IRIS we are analyzing only tetraspanin-marked subpopulations. It should be noted that different populations among the studied methods that may not express these markers could justify the greater efficiency in the transcriptomic, proteomic and glycomic results of ExoGAG.

Conclusions

In this study, we made a comparison between four EVs isolation methods from human milk (ExoGAG, IP_CD9, SEC and UC) and characterized the quantity and quality of proteins, RNA and miRNAs, and their potential applications in the field of proteomics, transcriptomics and glycomics.

We observed that ExoGAG improved, compared to the other techniques, the yield of total proteins and peptides, EVs-proteins and EVs-peptides, and glycosylated proteins. When developing proteomic functional analysis, we observed that ExoGAG and UC performed better

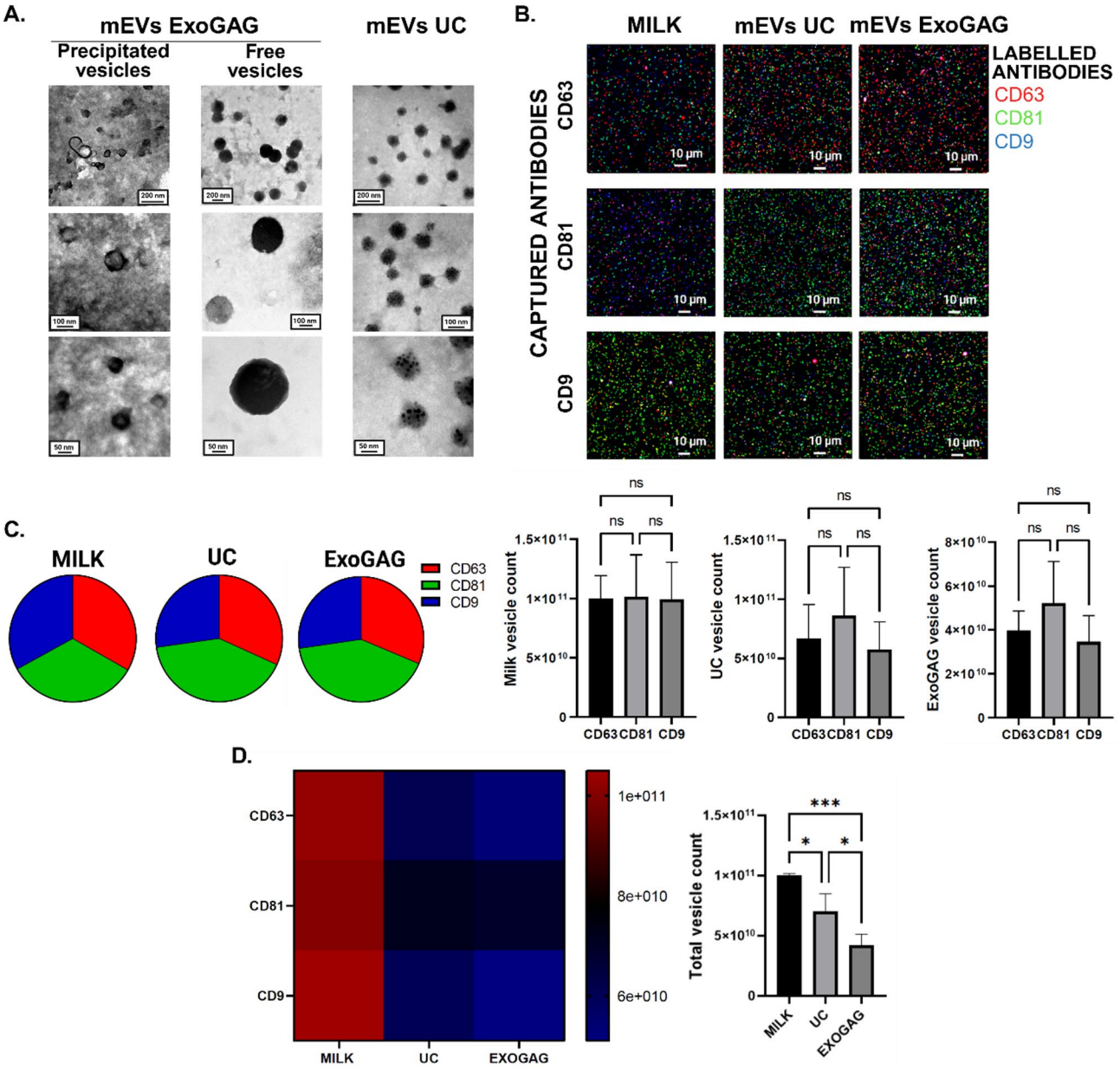

Fig. 10 Single-vesicle profile of raw milk and mEVs isolated by ExoGAG and Ultracentrifugation by TEM and SP-IRIS. **(A)** TEM images of mEVs derived from ExoGAG isolation method. We can see two types of EVs, precipitated forming part of the ExoGAG-GAG-Vesicle complex (the dye responsible for the complex would appear as a black background showing a dense image acquisition) or free, whereas UC mEVs only appear individually. (**B**) Immunofluorescence representative images of each condition showing vesicles captured and stained by CD63, CD81 and CD9. (**C**) Sectors graph and bar graph showing tetraspanin subpopulation profile (CD63 in red, CD81 in green and CD9 in blue) of raw milk, UC and ExoGAG mEVs. (**D**) Heatmap and bar graph representing differences between raw milk, ExoGAG and Ultracentrifugation isolation vesicle count. Bars represent means ± SEM. Ordinary One-way ANOVA was used for multiple comparisons and a value of $P < 0.05$ was considered significant. ns represents not significative, * $p < 0.05$, ** $p < 0.01$

(more sensitive), although the biological processes and enriched terms identified by all methods were similar (similar specificity). Regarding the functional mechanisms identified, we observed that human milk EVs contain proteins which are involved in the development of the infant, the maturation of the immune system and general and protein metabolism. ExoGAG also improves, with respect to the other techniques, the protein and peptide N-glycopatterns. IP_CD9 and UC lose the fucosialylated fraction and SEC and IP_CD9 isolate a lower proportion of fucosylated proteins, compared to UC and ExoGAG. Overall, ExoGAG appears to provide a more complete EVs-glycofingerprint than that provided by other methods being as well more similar to that of raw milk.

The mEVs isolation methods IP_CD9 and SEC were substantially less efficient for RNA analysis, with purity ratios that did not meet quality requirements, than ExoGAG and UC, which showed higher concentrations and less inter-sample variability. As expected, the levels and expression profiles of miRNAs detected by IP_CD9 and SEC were significantly worse than UC and ExoGAG, with the last being the technique with higher miRNA detection and lower inter-sample variability. Moreover, the GO analysis showed a better miRNA enrichment with more sensitivity after ExoGAG isolation and unmasked the exact same specific biological processes and enriched terms as the proteomic analysis (metabolism, developmental biology, protein metabolism and immune response), corroborating the previous findings.

Since the results obtained by UC and ExoGAG show greater consistency and reproducibility in proteomic and transcriptomic studies on the same sample, we tested their accuracy and reliability in the specific isolation of the vesicular component. First, we identified five EVs markers by Western Blot (CD9, CD81, ALIX, TSG101 and MFGE8) included in three different categories according to MISEV2023 classification and tested the removal of possible contaminants associated with the nature of the sample. Both techniques were equally comparable in the profile of characteristic NVEPs of raw milk (β-casein), results that can be significantly improved by using specific pretreatment methods for their removal if necessary. In contrast, NVEPs such as TGFBI were not detected in ExoGAG mEVs but were present in raw milk and UC mEVs, proving that ExoGAG unlike UC does not precipitate interferers. We also tested their removal capacity for other potential milk-specific contaminants, such as the lipid components of milk fat globules (MFG), like triglycerides and cholesterol [3]. In comparison to raw milk, both EVs isolation techniques were able to remove practically all triglycerides, and between 40% (UC) and 60% (ExoGAG) of cholesterol (also present in EVs surface). Both results together sustain that, with no previous chemical treatment, we were able to remove essentially all the fat globule from the samples only with the initial centrifugation steps.

Second, transmission electron microscopy images confirmed size and shape associated to vesicles, which must be between 30 nm and 1000 nm and have a circular form [31]. TEM images showed that ExoGAG is able to isolate two vesicular groups, forming a network-like complex between vesicles of different sizes associated with Glycosaminoglycans, and a second group formed by mostly large, individualized vesicles. In contrast, UC was able to isolate individualized vesicles mostly of small to medium size, which led us to think that it is more likely that this method is isolating a vesicular subpopulation, while ExoGAG is isolating a more complete vesicular profile, close to that of raw milk. SP-IRIS analysis was also developed to determine tetraspanin concentration and subpopulation profile. Both technologies showed a yield in the same order of magnitude, being better for UC tetraspanin interferometry, although not comparable with concentrations observed in the same raw milk used for isolation, as expected. The tetraspanin subpopulation profiles provided by both methods were practically equal, despite small differences in their concentration, indicating that the isolation methods do not introduce population biases based on the CD9, CD81 and CD63 markers. All conditions showed the same tendance where the major component was CD81, followed by CD63 and CD9. It should be noted also that different populations among the studied methods that may not express CD9, CD81 or CD63, could justify the greater efficiency in the transcriptomic, proteomic and glycomic results of ExoGAG.

So far, UC is the most used technique in the study of EVs, whose advantage is the consistency of the result but with the limitation of high sample volumes, time-consuming protocols and the requirement of expensive and specific equipment. ExoGAG is an EVs-specific aggregation isolation method that is just as efficient as UC for small sample volumes, with fast and easy-handling protocols and that requires the infrastructure commonly used in any laboratory. To conclude, both ExoGAG and UC exhibited a similar and high-quality ability to isolate EVs from human milk samples far superior to other standard techniques such as IP_CD9 or SEC. Moreover, the performance of ExoGAG was shown to be more efficient in terms of accuracy, consistency and reproducibility for proteomic, transcriptomic and glycomic studies on the same sample. This relies on ExoGAG improved isolation recovery of proteins and peptides, glycoproteins and RNA as well as miRNA expression related to vesicle complexes compared to UC. This study is the first to compare the reliability of four of the most commonly-used techniques for the isolation of extracellular vesicles in different omics with the same samples and in light of the results, proposes ExoGAG method for the isolation of vesicles in raw human milk for omics studies. Moreover, this comparative approach of four different EVs enrichment methods unanimously confirms that vesicular proteins in breast milk have implications in the infant in the defense system against external agents (specific role in the immune system pathway) and in the correct establishment of the neural structure (developmental pathway), while providing all the nutritional requirements for the correct growth of the newborn (metabolic pathway).

Abbreviations

(HM)	Human milk
(mEVs)	Milk extracellular vesicles
(EVs)	Extracellular vesicles

(UC)	Ultracentrifugation
(IP_CD9)	Immunoprecipitation with CD9
(SEC)	Size Exclusion Chromatography
(DLS)	Dynamic Light Scattering
(MS)	Mass spectrometry
(DDA-MS)	Data-dependent Acquisition
(SWATH-MS)	Sequential Window Acquisition of All Theoretical Fragment Ion Mass Spectra
(DEPs)	Differentially expressed proteins
(QC)	Quality control
(TEM)	Transmission electron microscopy
(SP-IRIS)	Single-particle interferometric reflectance imaging sensor
(MFG)	Milk fat globule
(MFGE8)	Milk fat globule epidermal growth factor 8
(MVBs)	Multivesicular bodies

Supplementary Information

The online version contains supplementary material available at https://doi.org/10.1186/s12964-025-02390-x.

Additional file 1: Supplementary Fig. 1. SWATH replicates analysis, Supplementary Fig. 2. DDA replicates analysis, Supplementary Fig. 4. Tables of TOP10 protein abundances based on areas under the curve (AUC) obtained with SWATH-MS detected in each isolation technique, Supplementary Fig. 4. Statistical analysis of total peptide and protein recovery and Venn Diagram and correlation matrix of SWATH-MS-detected proteins, Supplementary Fig. 5. Functional analysis of biological processes and enriched terms of SWATH-MS data with FunRich and Metascape tool, Supplementary Fig. 6. Interactions between proteins found in the DDA-MS analysis after isolation with the four methods, Supplementary Fig. 7. Gene ontology (GO) analysis of enriched terms after mEVs isolation with IP_CD9, Supplementary Fig. 8. Lipid profile of raw milk and mEVs isolated by ExoGAG and Ultracentrifugation.

Acknowledgements

The authors would like to acknowledge Health Research Institute of Santiago de Compostela (IDIS) and Clinical University Hospital (CHUS) for the facilities, equipment and materials provided to carry out the study as well as Instituto de Salud Carlos III (ISCIII) and Xunta de Galicia/GAIN for the funding.

Authors' contributions

MPH: Conceptualization, Data curation, Formal analysis, Investigation, Methodology, Validation, Visualization, Writing-original draft; RPL: Conceptualization, Investigation, Resources, Writing-review and editing; MEVM: Conceptualization, Investigation, Resources, Writing-review and editing; NLB: Methodology, Formal analysis, Supervision; PFG: Data curation, Formal analysis, Software; LLV: Data curation, Methodology; ABI: Methodology, Validation; LNG: Formal analysis, Methodology, Validation; SBB: Data curation, Methodology, Supervision, Writing-review & editing; MP: Investigation, Methodology, Resources, Supervision; MLC: Conceptualization, Investigation, Resources, Writing-review & editing; MAGG: Conceptualization, Funding acquisition, Investigation, Project administration, Resources, Supervision, Writing-review& editing.

Funding

This work was supported by; Instituto de Salud Carlos III (ISCIII) RICORS program to RICORS2040 (RD21/0005/0020 and RD24/0004/0010) funded by European Union – NextGenerationEU, Mecanismo para la Recuperación y la Resiliencia (MRR). Cofinanciado por la Unión Europea: Instituto de Carlos III (ISCIII) through the projects "PI15/01467", "PI18/0037" y "PI22/00227" and cofunded by the European Union: PMP21-00109 funded by the Instituto de Salud Carlos III (ISCIII): Senefro foundation (SEN2021_2): Xunta de Galicia/GAIN (Grupos con potencial de crecemento-GPC fund IN607B2023/07: Grant Invest AEP 2020. GAIN (Agencia Gallega de Innovación); Award number: IN607B2021_04.

Data availability

The datasets supporting the conclusions of this article are available in the ProteomeXchange Consortium via the PRIDE (Perez-Riverol et al., 2025) partner repository, with the dataset identifier PXD060683. We have submitted all relevant data of our experiments to the EV-TRACK knowledgebase (EV-TRACK ID: EV250090) (Van Deun J, et al. EV-TRACK: transparent reporting and centralizing knowledge in extracellular vesicle research. Nature methods. 2017;14(3):228-32).

Declarations

Ethics approval and informed consent to participate

The participating mothers gave their written informed consent to participate in this study. Ethics committee approval was obtained from Research Ethics Committees of Galicia (register code: 2020/243).

Competing interests

Only Miguel A. Garcia Gonzalez reports conflict of interest as is included as author in the patent of the isolation method KITGAG (Commercialized as ExoGAG).

Author details

[1]Group of Genetics and Developmental Biology of Renal Disease, Laboratory of Nephrology, Health Research Institute of Santiago de Compostela (IDIS), Clinical University Hospital (CHUS), Santiago de Compostela 15706, Spain
[2]Genomic Medicine Group, Clinical University Hospital (CHUS), Santiago de Compostela 15706, Spain
[3]RICORS2040 (Kidney Disease), ISCIII, Santiago de Compostela 15706, Spain
[4]Neonatology Department. Metabolic Unit, RICORS-SAMID, CIBERER. University Clinical Hospital of Santiago de Compostela, Santiago de Compostela 15706, Spain
[5]Obesidomic Group, Endocrinology Area, Health Research Institute of Santiago de Compostela (IDIS), Clinical University Hospital (CHUS)/ SERGAS, Santiago de Compostela 15706, Spain
[6]CIBER Pathophysiology Obesity and Nutrition, Instituto de Salud Carlos III, Madrid, Spain
[7]SP-IRIS Platform, Health Research Institute of Santiago de Compostela (IDIS), Clinical University Hospital (CHUS)/SERGAS, Santiago de Compostela, Spain
[8]Proteomic Platform, Health Research Institute of Santiago de Compostela (IDIS), Clinical University Hospital (CHUS), Santiago de Compostela 15706, Spain

Received: 14 March 2025 / Accepted: 6 August 2025
Published online: 02 October 2025

References

1. Basak T, Bhat A, Malakar D, Pillai M, Sengupta S. In-depth comparative proteomic analysis of yeast proteome using iTRAQ and SWATH based MS. Mol Biosyst. 2015;11(8):2135–43. https://doi.org/10.1039/c5mb00234f.
2. Bhattacharya A, Hamilton AM, Furberg H, Pietzak E, Purdue MP, Troester MA, Hoadley KA, Love MI. An approach for normalization and quality control for NanoString RNA expression data. Brief Bioinform. 2021;22(3) bbaa163. https://doi.org/10.1093/bib/bbaa163
3. Blans K, Hansen MS, Sørensen Lv, Hvam ML, Howard KA, Möller A, Wiking L, Larsen LB, Rasmussen JT. Pellet-free isolation of human and bovine milk extracellular vesicles by size-exclusion chromatography. J Extracell Vesicles. 2017;6(1) 1294340. https://doi.org/10.1080/20013078.2017.1294340
4. Buratta S, Urbanelli L, Tognoloni A, Latella R, Cerrotti G, Emiliani C, Chiaradia E. (2023). Protein and Lipid Content of Milk Extracellular Vesicles: A Comparative Overview. In *Life* (Vol. 13, Issue 2) Page. 401. MDPI. https://doi.org/10.3390/life13020401
5. Buzás EI, Tóth E, Sódar BW, Szabó-Taylor K. Molecular interactions at the surface of extracellular vesicles. In: Seminars in Immunopathology, vol. 40. Springer; 2018. p. 453–64. https://doi.org/10.1007/s00281-018-0682-0.
6. Camino T, Lago-Baameiro N, Sueiro A, Bravo SB, Couto I, Santos FF, Baltar J, Casanueva FF, Pardo M. Brown adipose tissue sheds extracellular vesicles that carry potential biomarkers of metabolic and thermogenesis activity which are affected by high fat diet intervention. Int J Mol Sci. 2022;23(18) 10826. https://doi.org/10.3390/ijms231810826

7. Casado-Fernández L, Laso-García F, Piniella D, Gómez-de Frutos MC, Otero-Ortega L, Bravo SB, Fuentes-Gimeno B, Docando F, Alonso-López E, Ruiz-Ares G, Rodríguez-Pardo J, Rigual R, de Celis-Ruiz E, Hervás C, Díez-Tejedor E, Gutiérrez-Fernández M. & Alonso de Leciñana, M. (2024). The proteomic signature of circulating extracellular vesicles following intracerebral hemorrhage: Novel insights into mechanisms underlying recovery. *Neurobiology of Disease*, *201*. https://doi.org/10.1016/j.nbd.2024.106665
8. Cerezo-Magaña M, Bång-Rudenstam A, Belting M. The pleiotropic role of proteoglycans in extracellular vesicle mediated communication in the tumor microenvironment. In Seminars in Cancer Biology. 2020;62:99–107. https://doi.org/10.1016/j.semcancer.2019.07.001.
9. Chitti Sv, Gummadi S, Kang T, Shahi S, Marzan AL, Nedeva C, Sanwlani R, Bramich K, Stewart S, Petrovska M, Sen B, Ozkan A, Akinfenwa M, Fonseka P, Mathivanan S. Vesiclepedia 2024: an extracellular vesicles and extracellular particles repository. Nucleic Acids Res. 2024;52(D1):D1694-8. https://doi.org/10.1093/nar/gkad1007.
10. Chutipongtanate S, Morrow AL, Newburg DS. (2022). Human Milk Extracellular Vesicles: A Biological System with Clinical Implications. In *Cells* (Vol. 11, Issue 15) Page. 2345. MDPI. https://doi.org/10.3390/cells11152345
11. Clos-Sansalvador M, Monguió-Tortajada M, Roura S, Franquesa M, Borràs FE. Commonly used methods for extracellular vesicles' enrichment: implications in downstream analyses and use. Eur J Cell Biol. 2022;101(3)151227. https://doi.org/10.1016/j.ejcb.2022.151227
12. Cominetti O, Dayon L. Unravelling disease complexity: integrative analysis of multi-omic data in clinical research. Expert Rev Proteomics. 2025;22(4):149–62. https://doi.org/10.1080/14789450.2025.2491357.
13. Cordido A, Nunez-Gonzalez L, Martinez-Moreno JM, Lamas-Gonzalez O, Rodriguez-Osorio L, Perez-Gomez MV, Martin-Sanchez D, Outeda P, Chiaravalli M, Watnick T, Boletta A, Diaz C, Carracedo A, Sanz AB, Ortiz A, Garcia-Gonzalez MA. Tweak signaling pathway Blockade slows cyst growth and disease progression in autosomal dominant polycystic kidney disease. J Am Soc Nephrol. 2021;32(8):1913–32. https://doi.org/10.1681/ASN.2020071094.
14. Cordido A, Vizoso-Gonzalez M, Nuñez-Gonzalez L, Molares-Vila A, Chantada-Vazquez MDP, Bravo SB, Garcia-Gonzalez MA. Quantitative proteomic study unmasks fibrinogen pathway in polycystic liver disease. Biomedicines. 2022;10(2) 290. https://doi.org/10.3390/biomedicines10020290
15. Dalgaard LT, Sørensen AE, Hardikar AA, Joglekar Mv. The microRNA-29 family: role in metabolism and metabolic disease. Am J Physiol Cell Physiol (Vol. 2022;323(2):C367-77. https://doi.org/10.1152/ajpcell.00051.2022.
16. Desjardins P, Conklin D. NanoDrop microvolume quantitation of nucleic acids. J Visualized Experiments. 2010. 45, 2565. https://doi.org/10.3791/2565
17. Fondevila MF, Novoa E, Fernandez U, Dorta V, Parracho T, Kreimeyer H, Garcia-Vence M, Chantada-Vazquez MP, Bravo SB, Porteiro B, Cabaleiro A, Koning M, Senra A, Souto Y, Verheij J, Guallar D, Fidalgo M, Meijnikman AS, da Silva Lima N, Nogueiras R. Inhibition of hepatic p63 ameliorates steatohepatitis with fibrosis in mice. Mol Metabolism. 2024;85, 101962. https://doi.org/10.1016/j.molmet.2024.101962
18. Galley JD, Besner GE. (2020). The therapeutic potential of breast milk-derived extracellular vesicles. In *Nutrients* (Vol. 12, Issue 3) page 745. MDPI AG. https://doi.org/10.3390/nu12030745
19. Godoy Sanches PH, de Melo NC, Porcari AM, de Carvalho LM. Proteom Metabolomics Biology. 2024;13(11):848. https://doi.org/10.3390/biology13110848. Integrating Molecular Perspectives: Strategies for Comprehensive Multi-Omics Integrative Data Analysis and Machine Learning Applications in Transcriptomics,.
20. Gonzalez-Rellan MJ, Fernández U, Parracho T, Novoa E, Fondevila MF, da Silva Lima N, Ramos L, Rodríguez A, Serrano-Maciá M, Perez-Mejias G, Chantada-Vazquez P, Riobello C, Veyrat-Durebex C, Tovar S, Coppari R, Woodhoo A, Schwaninger M, Prevot V, Delgado TC, Nogueiras R. Neddylation of phosphoenolpyruvate Carboxykinase 1 controls glucose metabolism. Cell Metabol. 2023;35(9):1630-e16455. https://doi.org/10.1016/j.cmet.2023.07.003.
21. Gormley A, Garavito-Duarte Y, Kim SW. The role of milk oligosaccharides in enhancing intestinal microbiota, intestinal integrity, and immune function in pigs: A comparative review. Biology. 2024;13(9):663. https://doi.org/10.3390/biology13090663.
22. Hadley Wickham. (2016) ggplot2 Elegant Graphics for Data Analysis Second Edition. (n.d.). http://www.springer.com/series/6991
23. Harris CR, Millman KJ, van der Walt SJ, Gommers R, Virtanen P, Cournapeau D, Wieser E, Taylor J, Berg S, Smith NJ, Kern R, Picus M, Hoyer S, van Kerkwijk MH, Brett M, Haldane A, del Río JF, Wiebe M, Peterson P, Oliphant TE. Array programming with NumPy. In Nature. 2020;585(7825):357–62.
24. Heidinger M, Egle D, Piscuoglio S, Navarro-Aguadero MÁ, Sánchez S, Hergueta-Redondo M, Gallardo M, Barrio S, García-Peláez B, Molina-Vila MA, Maggi N, Eller S, Loesch RM, Alborelli J, Peinado I, Weber H, Weber P. Extracellular vesicle DNA extraction and sequencing in ancient serum samples from patients with breast cancer. Anticancer Res. 2024;44(7):2981–8. https://doi.org/10.21873/anticanres.17110.
25. Herrero C, de la Fuente A, Casas-Arozamena C, Sebastian V, Prieto M, Arruebo M, Abalo A, Colás E, Moreno-Bueno G, Gil-Moreno A, Vilar A, Cueva J, Abal M, Muinelo-Romay L. Extracellular vesicles-based biomarkers represent a promising liquid biopsy in endometrial cancer. Cancers. 2019;11(12) 2000. https://doi.org/10.3390/cancers11127452000
26. Herrero C, Ferreirós A, Pérez-Fentes D, León-Mateos L, López-López R, Abal M, Alonso-Alconada L. Extracellular vesicles' genetic cargo as noninvasive biomarkers in cancer: A pilot study using ExoGAG technology. Biomedicines. 2023;11(2) 404. https://doi.org/10.3390/biomedicines11020404
27. Iraci N, Leonardi T, Gessler F, Vega B, Pluchino S. Focus on extracellular vesicles: physiological role and signalling properties of extracellular membrane vesicles. Int J Mol Sci (Vol. 2016;17(2) 171. MDPI AG. https://doi.org/10.3390/ijms17020171
28. Jiang X, You L, Zhang Z, Cui X, Zhong H, Sun X, Ji C, Chi X. (2021). Biological Properties of Milk-Derived Extracellular Vesicles and Their Physiological Functions in Infant. In *Frontiers in Cell and Developmental Biology* (Vol. 9) Page 693534. Frontiers Media S.A . https://doi.org/10.3389/fcell.2021.693534
29. Kahn S, Liao Y, Du X, Xu W, Li J, Lönnerdal B. Exosomal MicroRNAs in milk from mothers delivering preterm infants survive in vitro digestion and are taken up by human intestinal cells. Mol Nutr Food Res. 2018;62(11)e1701050. https://doi.org/10.1002/mnfr.201701050
30. Kluyver T, Ragan-Kelley B, Pérez F, Granger B, Bussonnier M, Frederic J, Kelley K, Hamrick J, Grout J, Corlay S, Ivanov P, Avila D, Abdalla S, Willing C. Jupyter Notebooks—a publishing format for reproducible computational workflows. Position Power Acad Publishing: Players Agents Agendas - Proc 20th Int Conf Electron Publishing ELPUB 2016. 2016;2016:87–90. https://doi.org/10.3233/978-1-61499-649-1-87.
31. Lässer C, Jang SC, Lötvall J. Subpopulations of extracellular vesicles and their therapeutic potential. Mol Aspects Med. 2018;60:1–14. https://doi.org/10.1016/j.mam.2018.02.002.
32. Li Y, Zhang R, Hei H. Advances in post-translational modifications of proteins and cancer immunotherapy. In *Frontiers in immunology*. Front Media SA. 2023;14,1229397. https://doi.org/10.3389/fimmu.2023.1229397
33. Li P, Chen P, Zheng Y, Suo G, Shen F, Li H, Zhong X, Chen X, Wu Y. Enhancement of motor neuron development and function in zebrafish by sialyllacto-N-tetraose b. Translational Pediatr. 2024a;13(7):1201–9. https://doi.org/10.21037/tp-24-247.
34. Li Y, Wang J, Chen W, Lu H, Zhang Y. (2024b). Comprehensive review of MS-based studies on N-glycoproteome and N-glycome of extracellular vesicles. In *Proteomics* (Vol. 24, Issue 11) Page. e2300065 . John Wiley and Sons Inc. https://doi.org/10.1002/pmic.202300065
35. Li Y, Zhang J, Inc. Animal models of stroke. In Animal Models and Experimental Medicine. John Wiley and Sons Inc. 2021;4(3):204–19. https://doi.org/10.1002/ame2.12179.
36. Ling ZN, Jiang YF, Ru JN, Lu JH, Ding B, Wu J. Amino acid metabolism in health and disease. In *Signal transduction and targeted therapy*. Issue 1) Springer Nat. 2023;8,345. https://doi.org/10.1038/s41392-023-01569-3
37. López-Valverde L, Vázquez-Mosquera ME, Colón-Mejeras C, Bravo SB, Barbosa-Gouveia S, Álvarez JV, Sánchez-Martínez R, López-Mendoza M, López-Rodríguez M, Villacorta-Argüelles E, Goicoechea-Diezhandino MA, Guerrero-Márquez FJ, Ortolano S, Leao-Teles E, Hermida-Ameijeiras Á, Couce ML. Characterization of the plasma proteomic profile of Fabry disease: potential sex- and clinical phenotype-specific biomarkers. Translational Res. 2024;269:47–63. https://doi.org/10.1016/j.trsl.2024.02.006.
38. Love MI, Huber W, Anders S. Moderated Estimation of fold change and dispersion for RNA-seq data with DESeq2. Genome Biol. 2014;15(12)550. https://doi.org/10.1186/s13059-014-0550-8
39. Ludwig C, Gillet L, Rosenberger G, Amon S, Collins BC, Aebersold R. Data-independent acquisition-based SWATH - MS for quantitative proteomics: a tutorial. Mol Syst Biol. 2018;14(8)e8126. https://doi.org/10.15252/msb.20178126
40. Lv LL, Feng Y, Tang TT, Liu BC. New insight into the role of extracellular vesicles in kidney disease. J Cell Mol Med (Vol. 2019;23(2):731–9. https://doi.org/10.1111/jcmm.14101. Blackwell Publishing Inc.
41. Manterola C, Grande L, Otzen T, García N, Salazar P, Quiroz G. (2018). Reliability, precision or reproducibility of the measurements. Methods of assessment,

utility and applications in clinical practice. *Revista chilena de Infectología*. www.sochinf.cl. Page 680-688.
42. Mather IH, Keenan TW. Origin and secretion of milk lipids. J Mammary Gland Biol Neoplasia. 1998;3(3):259–73. https://doi.org/10.1023/a:1018711410270.
43. McMahon DJ, Oommen BS. Supramolecular structure of the casein micelle. J Dairy Sci. 2008;91(5):1709–21. https://doi.org/10.3168/jds.2007-0819.
44. Mercadal M, Herrero C, López-Rodrigo O, Castells M, Fuente A, de la, Vigués F, Bassas L, Larriba S. Impact of extracellular vesicle isolation methods on downstream Mirna analysis in semen: A comparative study. Int J Mol Sci. 2020;21(17):1–18. https://doi.org/10.3390/ijms21175949.
45. Mukhopadhya A, Santoro J, O'Driscoll L. Extracellular vesicle separation from milk and infant milk formula using acid precipitation and ultracentrifugation. STAR Protocols. 2021;2(4)100821. https://doi.org/10.1016/j.xpro.2021.100821
46. Nakatani H, Aoki N, Nakagawa Y, Jin-No S, Aoyama K, Oshima K, Ohira S, Sato C, Nadano D, Matsuda T. Weaning-induced expression of a milk-fat globule protein, MFG-E8, in mouse mammary glands, as demonstrated by the analyses of its mRNA, protein and phosphatidylserine-binding activity. Biochem J. 2006;395(1):21–30. https://doi.org/10.1042/BJ20051459.
47. Perez-Riverol Y, Bandla C, Kundu DJ, Kamatchinathan S, Bai J, Hewapathirana S, John NS, Prakash A, Walzer M, Wang S, Vizcaíno JA. The PRIDE database at 20 years: 2025 update. Nucleic Acids Res. 2025;53(D1):D543–53. https://doi.org/10.1093/nar/gkae1011.
48. Picáns-Leis R, Vázquez-Mosquera ME, Pereira-Hernández M, Vizoso-González M, López -Valverde L, Barbosa-Gouveia S, López-Suárez O, López-Sanguos C, Bravo SB, García-González MA, Couce ML. Characterization of the functional component in human milk and identification of the molecular mechanisms undergoing prematurity. Clin Nutr. 2025;44:178–92. https://doi.org/10.1016/j.clnu.2024.12.013.
49. Raposo G, Stoorvogel W. Extracellular vesicles: exosomes, microvesicles, and friends. J Cell Biology (Vol. 2013;200:373–83. https://doi.org/10.1083/jcb.201211138.
50. Risso D, Ngai J, Speed TP, Dudoit S. Normalization of RNA-seq data using factor analysis of control genes or samples. Nat Biotechnol. 2014;32(9):896–902. https://doi.org/10.1038/nbt.2931.
51. Rodrigues JS, Chenlo M, Bravo SB, Perez-Romero S, Suarez-Fariña M, Sobrino T, Sanz-Pamplona R, González-Prieto R, Blanco Freire MN, Nogueiras R, López M, Fugazzola L, Cameselle-Teijeiro JM, Alvarez Cv. dsRNAi-mediated Silencing of PIAS2beta specifically kills anaplastic carcinomas by mitotic catastrophe. Nat Commun. 2024;15(1)3736. https://doi.org/10.1038/s41467-024-47751-1
52. Royo F, Cossío U, De Angulo R, Llop A, J., Falcon-Perez JM. Modification of the glycosylation of extracellular vesicles alters their biodistribution in mice. Nanoscale. 2019;11(4):1531–7. https://doi.org/10.1039/c8nr03900c.
53. Salehi M, Negahdari B, Mehryab F, Shekari F. Milk-Derived Extracellular Vesicles: Biomedical Applications, Current Challenges, and Future Perspectives. In Journal of Agricultural and Food Chemistry. American Chemical Society. 2024;72(15):8304–31. https://doi.org/10.1021/acs.jafc.3c07899.
54. Shevchenko A, Wilm M, Jensen N, Podtelejnikov Av, Neubauer G, Shevchenko A, Mortensen P, Mann M. (1996). Biochemical Mass SDectrometrv A strategy for identifying gel-separated proteins in sequence databases by MS alone. 24930, 24(3);893-896. https://doi.org/10.1042/bst0240893
55. Tenenbaum M, Deracinois B, Dugardin C, Matéos A, Romelard A, Auger J, Boulier A, Ravallec R, Flahaut C, Cudennec B. (2022). Identification, production and bioactivity of casein phosphopeptides – A review. In *Food Research International* (Vol. 157) Page.111360. Elsevier Ltd. https://doi.org/10.1016/j.foodres.2022.111360
56. Than UTT, Guanzon D, Broadbent JA, Leavesley DI, Salomon C, Parker TJ. Differential expression of keratinocyte-derived extracellular vesicle Mirnas discriminate exosomes from apoptotic bodies and microvesicles. Front Endocrinol. 2018;9, 535(SEP). https://doi.org/10.3389/fendo.2018.00535
57. Tiszbein K, Koss-Mikołajczyk I, Martysiak-Żurowska D. (2025). Unlocking the Secrets of Human Milk: Isolation and Characterization of Extracellular Vesicles. In Advances in Nutrition (Vol. 16, Issue 6) Page. 100430. Elsevier B.V. https://doi.org/10.1016/j.advnut.2025.100430
58. van Winkle LJ. (2001). Amino Acid Transport Regulation and Early Embryo Development. In *BIOLOGY OF REPRODUCTION* (Vol. 64) Page 1-12. http://www.biolreprod.org
59. Venable JD, Dong MQ, Wohlschlegel J, Dillin A, Yates JR. Automated approach for quantitative analysis of complex peptide mixtures from tandem mass spectra. Nat Methods. 2004;1(1):39–45. https://doi.org/10.1038/nmeth705.
60. Verhasselt V. (2024). A newborn's perspective on immune responses to food. In *Immunological Reviews*. John Wiley and Sons Inc. Page 117-129. https://doi.org/10.1111/imr.13376
61. Wang B. Molecular mechanism underlying Sialic acid as an essential nutrient for brain development and cognition. Adv Nutr. 2012;3(3)465S-472S. https://doi.org/10.3945/an.112.001875
62. Wang X, Li H, Wang Z, Chen J, Chen W, Zhou X, Zhang L, Xu S, Gao XD, Yang G. Site- and Structure-Specific glycosylation signatures of bovine, caprine, porcine, and human Milk-Derived extracellular vesicles. J Agric Food Chem. 2023;71(51):20826–37. https://doi.org/10.1021/acs.jafc.3c06439.
63. Welsh JA, Goberdhan DCI, O'Driscoll L, Buzas EI, Blenkiron C, Bussolati B, Cai H, di Vizio D, Driedonks TAP, Erdbrügger U, Falcon-Perez JM, Fu QL, Hill AF, Lenassi M, Lim SK, Mahoney MŸG, Mohanty S, Möller A, Nieuwland R, Zubair H. Minimal information for studies of extracellular vesicles (MISEV2023): from basic to advanced approaches. J Extracell Vesicles. 2024;13(2)e12404. https://doi.org/10.1002/jev2.12404
64. Xiang H, Zhang C, Xiong J. (2022). Emerging role of extracellular vesicles in kidney diseases. In *Frontiers in Pharmacology* (Vol. 13). Frontiers Media S.A. Page 985030. https://doi.org/10.3389/fphar.2022.985030
65. Xu S, Chen M, Feng T, Zhan L, Zhou L, Yu G. Use Ggbreak to effectively utilize plotting space to deal with large datasets and outliers. Front Genet. 2021;12,774846. https://doi.org/10.3389/fgene.2021.774846
66. Yáñez-Mó M, Siljander PRM, Andreu Z, Zavec AB, Borràs FE, Buzas EI, Buzas K, Casal E, Cappello F, Carvalho J, Colás E, Cordeiro-Da Silva A, Fais S, Falcon-Perez JM, Ghobrial IM, Giebel B, Gimona M, Graner M, Gursel I, de Wever O. Biological properties of extracellular vesicles and their physiological functions. In Journal of Extracellular Vesicles. 2015;4(2015):1–60. https://doi.org/10.3402/jev.v4.27066.
67. Yang YH, Wen R, Yang N, Zhang TN, Liu CF. (2023). Roles of protein post-translational modifications in glucose and lipid metabolism: mechanisms and perspectives. In *Molecular Medicine* (Vol. 29, Issue 1) Page 93. BioMed Central Ltd. https://doi.org/10.1186/s10020-023-00684-9
68. Yang Y, Wu J, Zhou W, Ji G, Dang Y. Protein posttranslational modifications in metabolic diseases: basic concepts and targeted therapies. MedComm. 2024;5(10)e752. https://doi.org/10.1002/mco2.752
69. Zafar S, Fatima SI, Schmitz M, Zerr I. (2024). Current Technologies Unraveling the Significance of Post-Translational Modifications (PTMs) as Crucial Players in Neurodegeneration. In *Biomolecules* (Vol. 14, Issue 1). Multidisciplinary Digital Publishing Institute (MDPI). https://doi.org/10.3390/biom14010118 Zhang, W., Zhou, X., Zhang, H., Yao, Q., Liu, Y., & Dong, Z. (2016). Extracellular vesicles in diagnosis and therapy of kidney diseases. *Am J Physiol Renal Physiol*, *311*, 844–851. https://doi.org/10.1152/ajprenal.00429.2016.-Extracel.
70. Zhong Y, Wang X, Zhao X, Shen J, Wu X, Gao P, Yang P, Chen J, An W. (2023). Multifunctional Milk-Derived Small Extracellular Vesicles and Their Biomedical Applications. In *Pharmaceutics* (Vol. 15, Issue 5) Page 1418. MDPI. https://doi.org/10.3390/pharmaceutics15051418
71. Zonneveld MI, Brisson AR, van Herwijnen MJC, Tan S, van de Lest CHA, Redegeld FA, Garssen J, Wauben MHM, Hoen EN. Recovery of extracellular vesicles from human breast milk is influenced by sample collection and vesicle isolation procedures. J Extracell Vesicles. 2014;3(1)24215. t. N. M. https://doi.org/10.3402/jev.v3.24215
72. Zuurveld M, van Witzenburg NP, Garssen J, Folkerts G, Stahl B, van't Land B, Willemsen LEM. (2020). Immunomodulation by Human Milk Oligosaccharides: The Potential Role in Prevention of Allergic Diseases. In *Frontiers in Immunology* (Vol. 11) Page 801. Frontiers Media S.A. https://doi.org/10.3389/fimmu.2020.00801

Publisher's Note